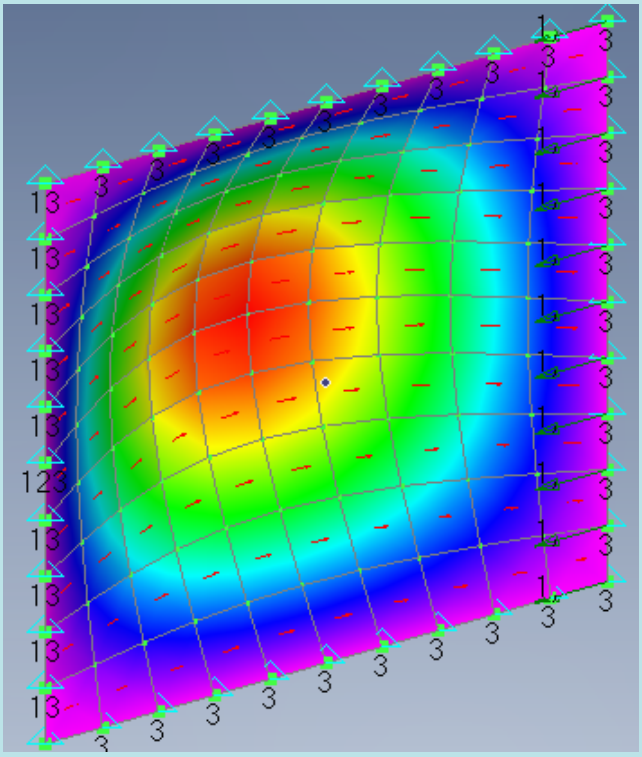

CA II with Matlab/Femap

Aerospace Structures Project (PART I)

Antonio Carotenuto

A.A 2024-2025

Contents

List of Figures

Chapter 1

Introduction

1.1 Composite Materials

Composite materials are materials consisting of two or more components with different physical or chemical properties, combined to obtain a material with characteristics superior to the individual components. These materials are often used to combine advantages such as strength, lightness, hardness, or flexibility, and find applications in sectors like the aerospace, automotive, construction, and sports industries. A common example is the carbon fiber composite, which combines the strength of the fiber with the lightness of the polymer matrix. Composite materials have been used for over a century, but their widespread use and application have intensified mainly over the last 70 years. The use of composites dates back to the early 1900s, with the combination of materials like wood and metal, but it was during World War II that the potential of composites began to be seriously exploited, particularly for aeronautical applications.

Initially, there was some skepticism towards composite materials, due to the perception that they were difficult to produce uniformly and did not possess the same reliability as traditional materials like metals and wood. Their strength and durability were difficult to test, and large-scale production was costly and complex.

Over the years, thanks to advancements in manufacturing technologies, such as the polymerization of composites and the introduction of advanced techniques like carbon fiber and glass fiber, these materials have gained trust. Modern technologies have enabled more precise production and greater accessibility, lowering costs and making composites more competitive compared to conventional materials. In the aeronautical field, regulatory specifications, which require rigorous certification and thorough testing, contributed to limiting the adoption of composite materials in aeronautics for a long time. Only with the development of more advanced production methods, the adoption of more precise quality control techniques, and the accumulation of reliable data on the behavior of composites under extreme operating conditions, was it possible to obtain approval for their increasingly widespread use. However, due to the risks associated with their processing and potential difficulties in detecting invisible damage (such as microcracks), regulations remain particularly strict for the aerospace industry.

A composite material is generally constituted by plies (often called plies). Each plies is a layer composed of fibers and the matrix. Fibers play a fundamental role in determining the strength and stiffness of composites: fiber-reinforced materials are much stronger in the direction of the fibers compared to the pure polymer, but the stiffness is less pronounced in the perpendicular direction. For this reason, fibers are often arranged in different directions, creating complex and adaptable structures that enhance the material's robustness. In a composite, fibers are combined with a substance called the "matrix". Although it might seem counterintuitive to mix high-strength fibers with polymers, the matrix serves as a binder to hold the fibers together and allow them to withstand compressive loads. Furthermore, the matrix facilitates load distribution among the fibers, preventing excessive stress on individual filaments. The matrix also plays an important role in determining the composite's response to external factors such as moisture, chemical agents, and UV rays, as well as influencing surface appearance, color, and fire safety.

Composites are classified based on the type of fiber used. Long (or continuous) fibers: The fibers extend throughout the entire length of the component and are arranged in an oriented manner (unidirectional or multidirectional). They offer high strength and stiffness but are more expensive and complex to produce.

Short (or discontinuous) fibers: The fibers are shorter and distributed randomly or in an oriented manner. They are easier and cheaper to produce but offer lower strength compared to long fibers. They are used in simpler, less critical components, such as in the automotive sector and reinforced plastics.

In the aerospace field, laminates with plies of long unidirectional fibers are widespread, meaning a composite material consisting of multiple superimposed layers, where each ply is characterized by continuous fibers oriented in the same direction. The plies are stacked on top of each other with different orientations to balance the mechanical properties of the material. For example, a laminate might have alternating layers with fibers arranged at 0°, 90°, 45°, and -45° to achieve balanced strength in all directions. In general, the design of these laminates involves careful placement of the layers to optimize mechanical properties based on the expected stresses.

In all subsequent chapters of this work, reference will always be made to this latter type of composite material. The discussion will focus on the development of MATLAB codes and FEM models, aimed at performing various analyses in parallel with the application of concepts learned during the Costruzioni II course.

1.2 Stress-Strain Relationship in the ply

Composite laminates are anisotropic materials: their mechanical properties vary depending on the direction of stress. For anisotropic materials, the stress-strain relationship can be described by the generalized Hooke's law (1.1), (1.2):

$$\begin{Bmatrix} \sigma_1 \\ \sigma_2 \\ \sigma_3 \\ \tau_4 \\ \tau_5 \\ \tau_6 \end{Bmatrix} = \begin{Bmatrix} C_{11} & C_{12} & C_{13} & C_{14} & C_{15} & C_{16} \\ C_{21} & C_{22} & C_{23} & C_{24} & C_{25} & C_{26} \\ C_{31} & C_{32} & C_{33} & C_{34} & C_{35} & C_{36} \\ C_{41} & C_{42} & C_{43} & C_{44} & C_{45} & C_{46} \\ C_{51} & C_{52} & C_{53} & C_{54} & C_{55} & C_{56} \\ C_{61} & C_{62} & C_{63} & C_{64} & C_{65} & C_{66} \end{Bmatrix} \begin{Bmatrix} \varepsilon_1 \\ \varepsilon_2 \\ \varepsilon_3 \\ \gamma_4 \\ \gamma_5 \\ \gamma_6 \end{Bmatrix} \tag{1.1}$$

$$\begin{Bmatrix} \varepsilon_1 \\ \varepsilon_2 \\ \varepsilon_3 \\ \gamma_4 \\ \gamma_5 \\ \gamma_6 \end{Bmatrix} = \begin{bmatrix} S_{11} & S_{12} & S_{13} & S_{14} & S_{15} & S_{16} \\ S_{21} & S_{22} & S_{23} & S_{24} & S_{25} & S_{26} \\ S_{31} & S_{32} & S_{33} & S_{34} & S_{35} & S_{36} \\ S_{41} & S_{42} & S_{43} & S_{44} & S_{45} & S_{46} \\ S_{51} & S_{52} & S_{53} & S_{54} & S_{55} & S_{56} \\ S_{61} & S_{62} & S_{63} & S_{64} & S_{65} & S_{66} \end{bmatrix} \begin{Bmatrix} \sigma_1 \\ \sigma_2 \\ \sigma_3 \\ \tau_4 \\ \tau_5 \\ \tau_6 \end{Bmatrix} \tag{1.2}$$

In the first relation (1.1), C is called the "Stiffness Matrix"; in the second (1.2), S is called the "Compliance Matrix". Theoretically, they consist of 36 independent coefficients, but in cases of interest to us, Betti's Reciprocity Theorem applies, meaning the Stiffness matrix is symmetric, and only 21 coefficients are independent. There are also structures with particular material symmetry properties for which the number of independent constants is smaller. Orthotropic materials are materials that exhibit three mutually orthogonal planes of material symmetry. For these materials, there is no coupling between normal stresses (σ_1, σ_2,σ_3) and shear strains (γ_4, γ_5,γ_6), nor between shear stresses (τ_4, τ_5,τ_6) and normal strains (ε_1, ε_2, ε_3), nor between shear stresses in one plane and shear strains in another plane. (Note: Original text mentioned coupling between shear stress and normal strain, and shear stress in plane and strain out of plane, which is slightly different but the effect is similar - decoupling). Consequently, for these materials, the number of independent constants reduces from 21 to 9; examples include wood and some crystals. Then there are transversely isotropic materials, which are characterized by a plane of isotropy. plies with long unidirectional fibers are an example of these materials, as the ply's behavior is the same regardless of the stress direction, provided it lies in the plane normal to the fiber direction. For these materials, the number of independent elastic constants is 5. When studying plies, it is often assumed that both the stress state and the strain state are planar (plane stress or plane strain). This is often justified by factors such as small thicknesses compared to other dimensions and the absence of significant transverse loads. Therefore, an approximation is made assuming a planar state, i.e., certain stress and/or strain components normal to the ply plane are considered zero or negligible. Under the common plane stress assumption ($\sigma_3 = \tau_4 = \tau_5 = 0$), the number of independent constants needed to describe the in-plane behavior becomes 4.

The stress-strain relationship for a ply under plane stress can be rewritten in the form:

$$\begin{bmatrix} \epsilon_1 \\ \epsilon_2 \\ \gamma_{12} \end{bmatrix} = \begin{bmatrix} S_{11} & S_{12} & 0 \\ S_{21} & S_{22} & 0 \\ 0 & 0 & S_{66} \end{bmatrix} \begin{bmatrix} \sigma_1 \\ \sigma_2 \\ \tau_{12} \end{bmatrix} \tag{1.3}$$

$$\begin{bmatrix} \epsilon_1 \\ \epsilon_2 \\ \gamma_{12} \end{bmatrix} = \begin{bmatrix} \frac{1}{E_1} & -\frac{\nu_{12}}{E_1} & 0 \\ -\frac{\nu_{21}}{E_2} & \frac{1}{E_2} & 0 \\ 0 & 0 & \frac{1}{G_{12}} \end{bmatrix} \begin{bmatrix} \sigma_1 \\ \sigma_2 \\ \tau_{12} \end{bmatrix} \tag{1.4}$$

In Eq. (1.4), E_1 is the "Elastic Modulus" (or Young's Modulus) in the local direction 1, E_2 is the Elastic Modulus in direction 2, G_{12} is the "Shear Modulus", and ν_{12} is the major

"Poisson's ratio" ($\nu_{12} = -\varepsilon_2/\varepsilon_1$ for uniaxial stress σ_1). Note that $S_{12} = -\nu_{12}/E_1 = S_{21} = -\nu_{21}/E_2$. Often, the inverse of the compliance matrix [S] in equation (1.4) is commonly denoted by [Q], the reduced stiffness matrix, in ply analysis, so the equation is also rewritten in the form:

$$\begin{bmatrix} \sigma_1 \\ \sigma_2 \\ \tau_{12} \end{bmatrix} = \begin{bmatrix} Q_{11} & Q_{12} & 0 \\ Q_{12} & Q_{22} & 0 \\ 0 & 0 & Q_{66} \end{bmatrix} \begin{bmatrix} \epsilon_1 \\ \epsilon_2 \\ \gamma_{12} \end{bmatrix} \tag{1.5}$$

where the elements are evaluated as:

$$Q_{11} = \frac{E_1}{1-\nu_{12}\nu_{21}}, \quad Q_{22} = \frac{E_2}{1-\nu_{12}\nu_{21}}, \quad Q_{12} = \frac{\nu_{12}E_2}{1-\nu_{12}\nu_{21}} = \frac{\nu_{21}E_1}{1-\nu_{12}\nu_{21}}, \quad Q_{66} = G_{12} \tag{1.6}$$

The written relations ((1.3), (1.4), (1.5)) are valid in the local reference frame (1-2) of the ply, where 1 generally indicates the fiber direction, and 2 indicates the transverse direction, as in Fig.1.1. However, what is often of interest is the study of the mechanical behavior of the entire laminate in a global coordinate system (x-y), in which the plies will be oriented differently. For this reason, it is necessary to introduce a single global reference frame, and the orientation of each ply can be represented by a single parameter θ, called the lamination angle (or ply angle), which corresponds to the angle measured counterclockwise from the x-axis of the global reference frame to the 1-axis of the local reference frame, as shown in Fig.1.2. The problem is to express the stress-strain relations of each ply in the global reference frame. This involves transforming the stress and strain tensors from one reference frame to another. For plane stress, this transformation can be derived by studying the equilibrium of an infinitesimal element, like the one shown conceptually in Fig.1.3. Using $c = \cos\theta$ and $s = \sin\theta$, the stress transformation relation is obtained:

$$\begin{Bmatrix} \sigma_x \\ \sigma_y \\ \tau_{xy} \end{Bmatrix} = \begin{bmatrix} c^2 & s^2 & 2sc \\ s^2 & c^2 & -2sc \\ -sc & sc & c^2-s^2 \end{bmatrix} \begin{Bmatrix} \sigma_1 \\ \sigma_2 \\ \tau_{12} \end{Bmatrix} \tag{1.7}$$

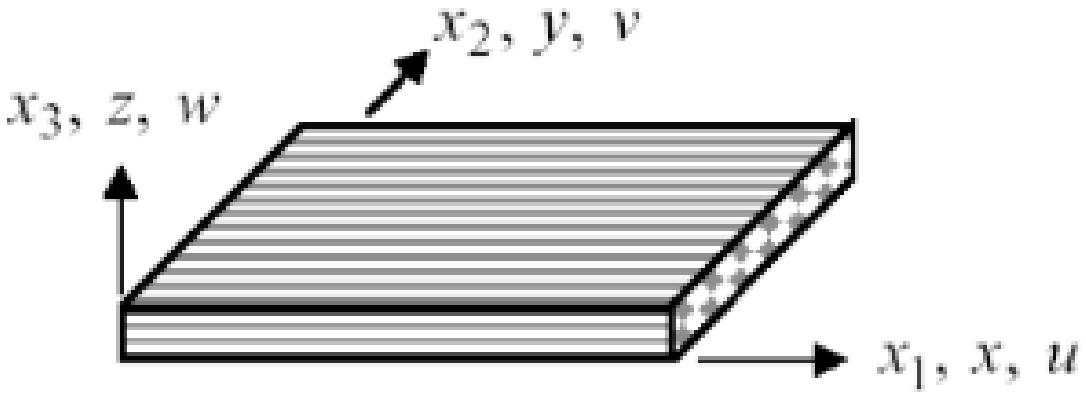

Figure 1.1 Local reference system (1-2) of the ply

In compact form:

$$\sigma_{xy} = T_\sigma \sigma_{12} \tag{1.8}$$

Similarly, it is possible to express the strain tensor transformation. For engineering strains $(\epsilon_x, \epsilon_y, \gamma_{xy})$:

$$\begin{Bmatrix} \epsilon_x \\ \epsilon_y \\ \gamma_{xy}/2 \end{Bmatrix} = \begin{bmatrix} c^2 & s^2 & sc \\ s^2 & c^2 & -sc \\ -2sc & 2sc & c^2 - s^2 \end{bmatrix} \begin{Bmatrix} \epsilon_1 \\ \epsilon_2 \\ \gamma_{12}/2 \end{Bmatrix} \tag{1.9}$$

Or using the Reuter matrix T_ϵ for engineering strain vector $\{\epsilon_x, \epsilon_y, \gamma_{xy}\}$:

$$\begin{Bmatrix} \epsilon_x \\ \epsilon_y \\ \gamma_{xy} \end{Bmatrix} = T_\epsilon \begin{Bmatrix} \epsilon_1 \\ \epsilon_2 \\ \gamma_{12} \end{Bmatrix} \quad \text{where} \quad T_\epsilon = \begin{bmatrix} c^2 & s^2 & sc \\ s^2 & c^2 & -sc \\ -2sc & 2sc & c^2 - s^2 \end{bmatrix} \tag{1.10}$$

From the preceding relations, one can derive the transformed reduced stiffness matrix $[\bar{Q}]$ for the ply in the global (x-y) reference frame:

$$[\bar{Q}] = T_\sigma^{-1}[Q]T_\epsilon \tag{1.11}$$

Alternatively, using the inverse relationship $\sigma_{12} = T_\sigma^{-1}\sigma_{xy}$ and $\epsilon_{12} = T_\epsilon^{-1}\epsilon_{xy}$ in $\sigma_{12} =$

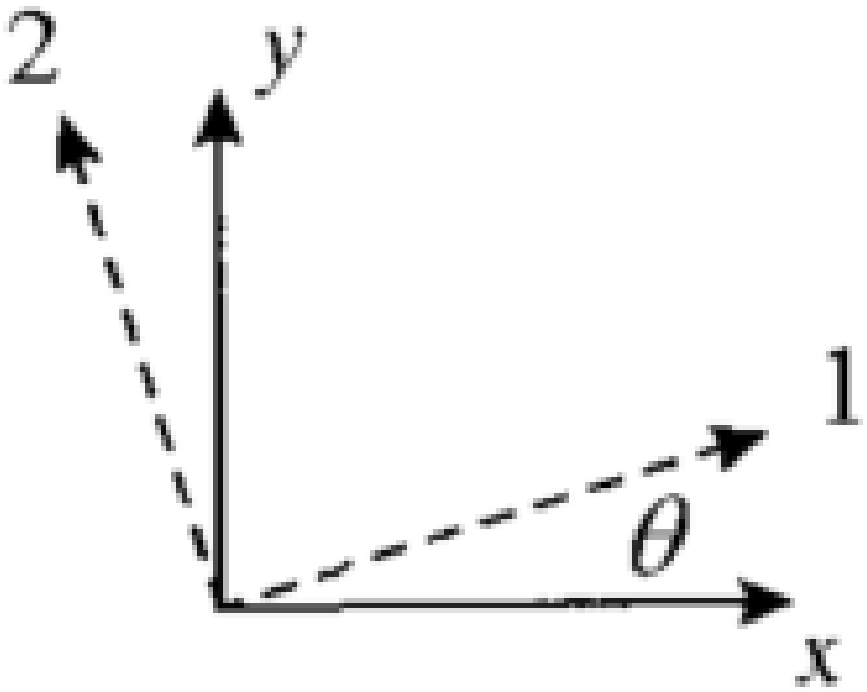

Figure 1.2 Relative orientation between local (1-2) and global (x-y) reference frames, lamination angle θ.

$[Q]\epsilon_{12}$, we get $\sigma_{xy} = T_\sigma[Q]T_\epsilon^{-1}\epsilon_{xy}$. So $[\bar{Q}] = T_\sigma[Q]T_\epsilon^{-1}$. It can be shown that $T_\epsilon^{-1} = T_\sigma^T$. Therefore:

$$[\bar{Q}] = T_\sigma[Q]T_\sigma^T \tag{1.12}$$

where $[\bar{Q}]$ relates global stresses and strains: $\{\sigma_x, \sigma_y, \tau_{xy}\}^T = [\bar{Q}]\{\epsilon_x, \epsilon_y, \gamma_{xy}\}^T$. Explicitly:

$$\begin{bmatrix} \bar{Q}_{xx} & \bar{Q}_{xy} & \bar{Q}_{xs} \\ \bar{Q}_{xy} & \bar{Q}_{yy} & \bar{Q}_{ys} \\ \bar{Q}_{xs} & \bar{Q}_{ys} & \bar{Q}_{ss} \end{bmatrix} = \left(T_\sigma^{-1}\right)^T \begin{bmatrix} Q_{11} & Q_{12} & 0 \\ Q_{12} & Q_{22} & 0 \\ 0 & 0 & Q_{66} \end{bmatrix} T_\sigma^{-1} \begin{bmatrix} \bar{Q}_{xx} & \bar{Q}_{xy} & \bar{Q}_{xs} \\ \bar{Q}_{xy} & \bar{Q}_{yy} & \bar{Q}_{ys} \\ \bar{Q}_{xs} & \bar{Q}_{ys} & \bar{Q}_{ss} \end{bmatrix} = T_\sigma^{-T} \begin{bmatrix} Q_{11} & Q_{12} & 0 \\ Q_{12} & Q_{22} & 0 \\ 0 & 0 & Q_{66} \end{bmatrix} T_\sigma^{-1} \tag{1.13}$$

1.3 Example Calculation of Stiffness and Compliance Matrices

A program written in MATLAB is presented, studying a panel made of Graphite/Epoxy BMS 8-212 Type II Class 1 composite material with properties shown in Table 1.1.

The code allows evaluating the transformed reduced Stiffness Matrix $[\bar{Q}]$ and the corresponding Compliance Matrix $[\bar{S}] = [\bar{Q}]^{-1}$ as the lamination angle θ varies. Specifically, the effective engineering constants in the global (x-y) coordinates, such as the effective

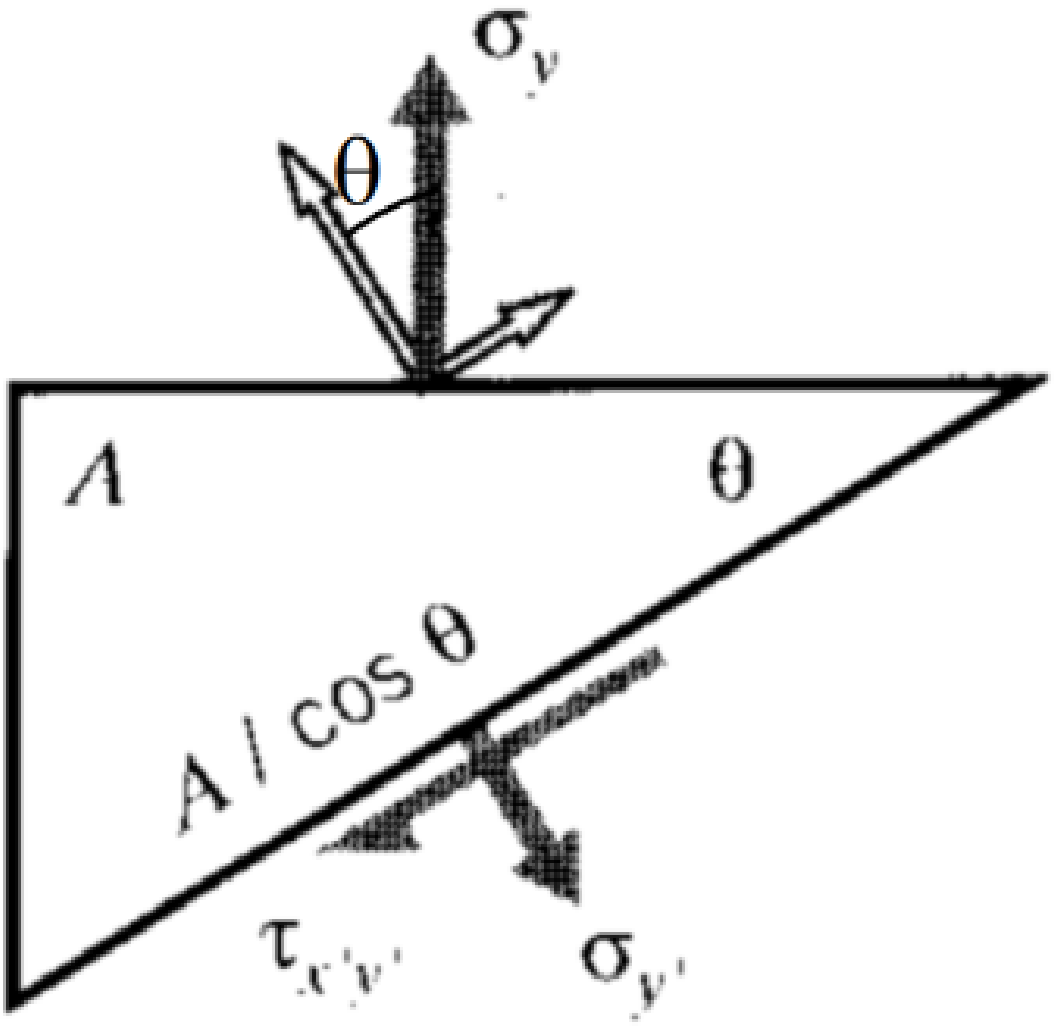

Figure 1.3 Equilibrium on an element for stress transformation.

Property	Value
E_1	125 GPa
E_2	12.5 GPa
G_{12}	6.89 GPa
ν_{12}	0.38
ν_{21}	0.038

Table 1.1 Material Properties

moduli E_x, E_y, G_{xy}, and the effective Poisson's ratio ν_{xy}, are evaluated as a function of the lamination angle. These can be calculated from the components of $[\bar{S}]$: $E_x = 1/\bar{S}_{11}$, $E_y = 1/\bar{S}_{22}$, $G_{xy} = 1/\bar{S}_{66}$, $\nu_{xy} = -\bar{S}_{12}/\bar{S}_{11}$. Often plots show normalized moduli like E_x/E_2, E_y/E_2, G_{xy}/G_{12} (or G_{xy}/E_2) and ν_{xy}.

Listing 1.1

```
E_1 = 125e9; %(Pa)
E_2 = 12.5e9; %(Pa)
nu_12 = 0.38;
G_12 = 6.89e9; %(Pa)
t = 0.15e-3; %(m)
L= 0.5; %(m)


%% matrice Q
Q_11 = E_1/(1-(E_2/E_1)*(nu_12)^2);
Q_12 = nu_12*E_2/(1-(E_2/E_1)*(nu_12)^2);
Q_22 = E_2/(1-(E_2/E_1)*(nu_12)^2);
Q_66 = G_12;

Q=[Q_11 Q_12 0;
    Q_12 Q_22 0;
    0 0 Q_66];

%% calcolo matrici di rotazione

T_sigma = @(theta) [(cos(theta))^2  (sin(theta))^2  -2*cos(theta)*sin(
    theta);
    (sin(theta))^2  (cos(theta))^2  2*cos(theta)*sin(theta);
    cos(theta)*sin(theta)  -cos(theta)*sin(theta)  (cos(theta))^2-(sin(
    theta))^2];


T_eps = @(theta) [(cos(theta))^2  (sin(theta))^2  -cos(theta)*sin(theta);
    (sin(theta))^2  (cos(theta))^2  cos(theta)*sin(theta);
    2*cos(theta)*sin(theta)  -2*cos(theta)*sin(theta)  (cos(theta))^2-(
    sin(theta))^2];



%% calcolo matrice Q nel riferimento globale e matrice S

Q_glob = @(theta) (T_sigma(theta) * Q) / T_eps(theta);

```

```
S_glob = @(theta) inv(Q_glob(theta));
```

The lines of code related to plotting have been omitted. Instead, the figures showing the results are reported in Fig.1.4, 1.5. (Assuming the plots show normalized moduli as described in the original text).

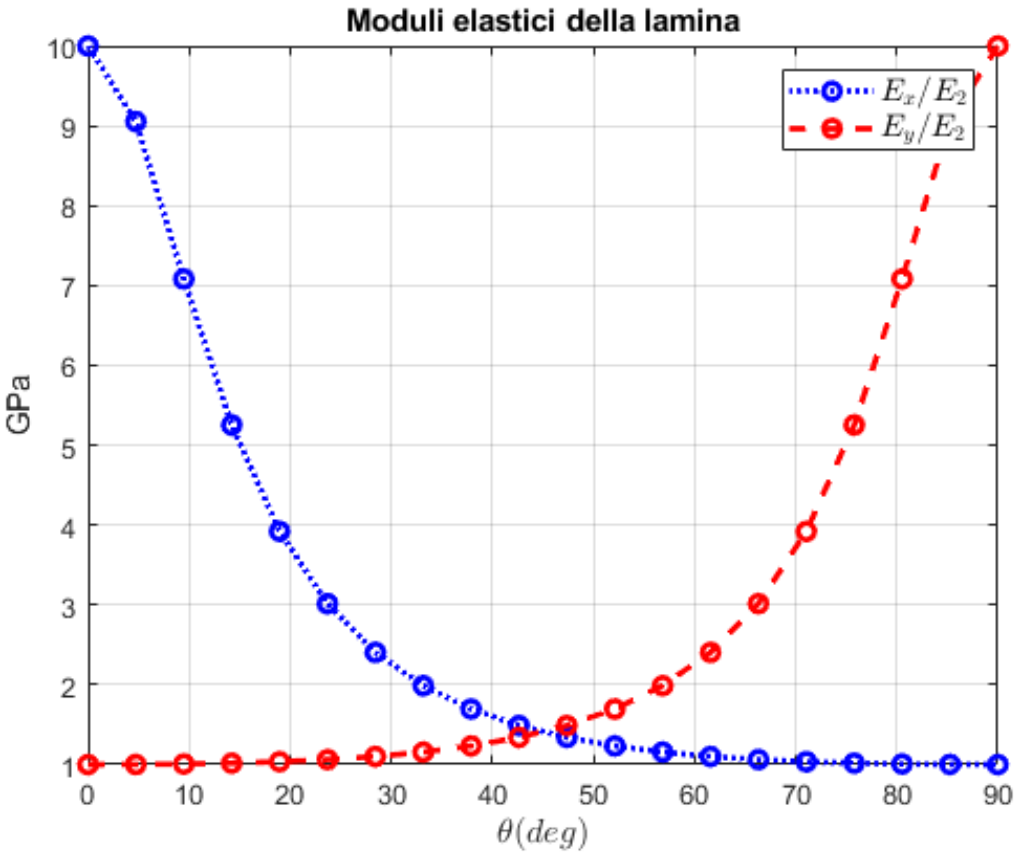

Figure 1.4 Variation of normalized elastic moduli (E_x/E_2, E_y/E_2) vs. lamination angle θ

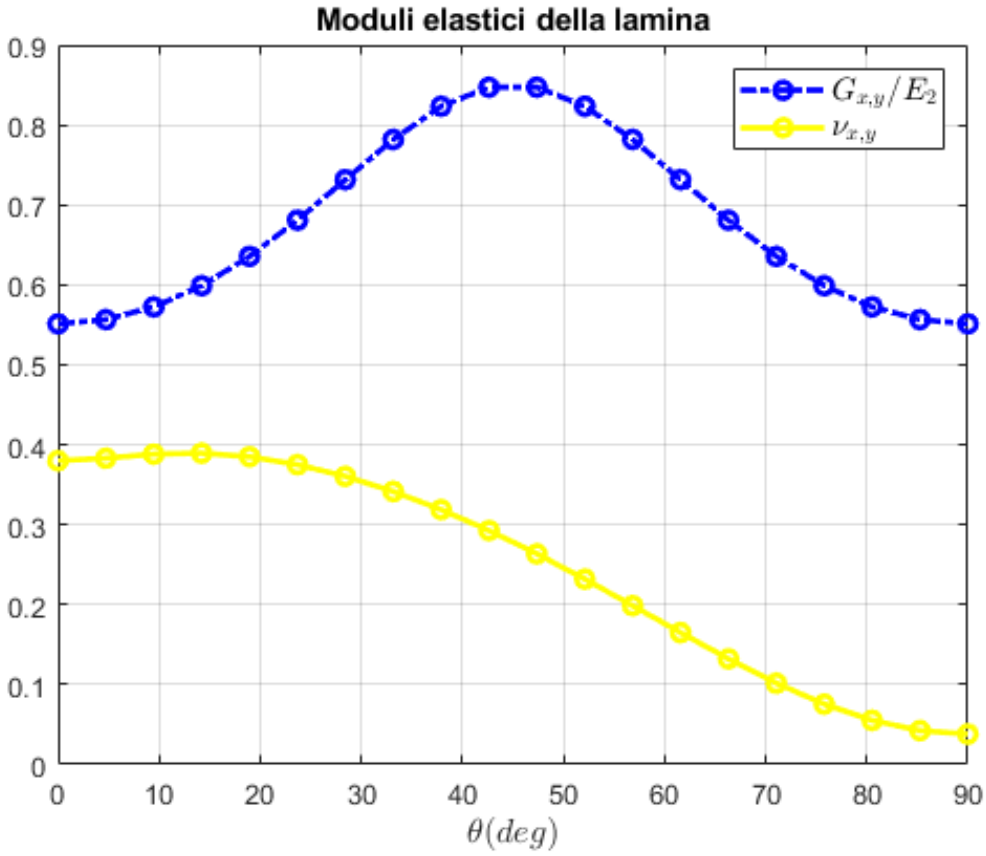

Figure 1.5 Variation of Poisson's ratio (ν_{xy}) and normalized shear modulus (G_{xy}/E_2) vs. lamination angle θ

Chapter 2

Classical Lamination Theory

2.1 Assumptions and Limitations in CLT

Classical Lamination Theory (CLT) is fundamental in the study of composite materials because it provides a simplified method for analyzing the mechanical behavior of laminated structures. According to this theory, a laminate consists of individual layers (plies), each with constant thickness, material properties, and orientation. The layers are bonded together to form a composite material. The assumptions underlying Classical Lamination Theory are:

- Homogeneity and Orthotropy: Each layer must be effectively homogeneous and orthotropic. "Effectively homogeneous" means that, at a macroscopic level, the layer can be treated as a homogeneous material, even though it is composed of multiple phases at the microscopic level.
- Laminate Thickness: The laminate must be much thinner in one direction compared to the other two. This allows treating it as a thin plate with equivalent properties representing the entire laminate, simplifying stiffness calculations.
- In-plane Stresses/Strains: Stresses act primarily within the plane of the laminate, implying a state of plane stress (or generalized plane strain), and strains are predominantly planar.
- Small Strains: Strains must be small compared to the laminate thickness (typically at least an order of magnitude smaller).
- Strain Continuity: Strains must be continuous throughout the entire laminate, indicating perfect bonding and no discontinuities (like slip) between layers, which are treated as a single structure.
- Negligible Transverse Shear Effects (Kirchhoff Hypothesis): Transverse shear strains (γ_{xz}, γ_{yz}) are negligible. This implies that lines initially normal to the mid-surface remain straight and normal to the deformed mid-surface after bending, without significant shear deformation effects.

- Negligible Normal Strain (ϵ_z): The through-the-thickness normal strain (ϵ_z) is negligible compared to the in-plane strains.
- Linear Relationships: The stress-strain and strain-displacement relationships must be linear (linear elasticity and small displacements/rotations). This is generally valid for small displacements and rotations.

Classical Lamination Theory (CLT), despite being very simple and working accurately in many cases of interest, has limitations:

- Neglect of Transverse Shear Deformation: CLT assumes zero transverse shear strains within the laminate. This is valid for thin laminates, but for thick laminates or those under high shear loads, this assumption can lead to inaccurate results (e.g., underestimation of deflections, overestimation of natural frequencies).
- Limitation to Thin Laminates: CLT is primarily applicable to thin laminates. In thick laminates, through-the-thickness shear deformation can be significant and is not considered by the theory, making the results less accurate.
- Neglect of Interlaminar Stresses: CLT does not inherently account for the stresses (σ_z, τ_{xz}, τ_{yz}) that develop between the different layers of a laminate, particularly near free edges or discontinuities. These stresses are important in predicting delamination or bond failure between layers, and their omission limits the applicability of CLT in such cases.
- Assumption of Linear Elasticity: CLT assumes that the laminate materials behave in a linear elastic manner, without changes in their mechanical parameters under load. However, in cases of high loads or materials exhibiting non-linear behavior, this assumption can lead to incorrect predictions.

Summary: Classical Lamination Theory is useful for analyzing thin composite laminates but has significant limitations for thick laminates, non-linear deformations, and interlaminar stresses. More advanced theories like the First-Order Shear Deformation Theory (FSDT) and Higher-Order Shear Deformation Theories (HSDT) have been developed to address these issues and provide more accurate results.

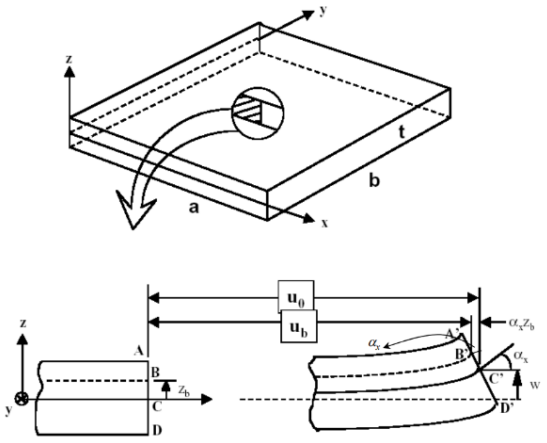

Figure 2.1 Displacements within the laminate (u, v, w).

2.2 Equations in Classical Lamination Theory

In this section, the equations of Classical Lamination Theory are developed based on the assumptions discussed in the previous section. Using the hypothesis of small strains and linearity, the strain-displacement relationship can be written based on the Kirchhoff hypothesis for plates. The displacements u, v, w at a point (x, y, z) are related to the mid-plane displacements u_0, v_0, w_0 (where $w_0 = w(x, y, 0)$) as: $u(x, y, z) = u_0(x, y) - z\frac{\partial w_0}{\partial x}$ $v(x, y, z) = v_0(x, y) - z\frac{\partial w_0}{\partial y}$ $w(x, y, z) = w_0(x, y)$ The non-zero strains are then:

$$\begin{aligned}
\varepsilon_x &= \frac{\partial u}{\partial x} = \frac{\partial u_0}{\partial x} - z\frac{\partial^2 w_0}{\partial x^2} \\
\varepsilon_y &= \frac{\partial v}{\partial y} = \frac{\partial v_0}{\partial y} - z\frac{\partial^2 w_0}{\partial y^2} \\
\gamma_{xy} &= \frac{\partial u}{\partial y} + \frac{\partial v}{\partial x} = \left(\frac{\partial u_0}{\partial y} + \frac{\partial v_0}{\partial x}\right) - 2z\frac{\partial^2 w_0}{\partial x \partial y} \\
\varepsilon_z &= \gamma_{xz} = \gamma_{yz} = 0
\end{aligned} \tag{2.1}$$

where the terms with subscript 0 represent properties of the mid-plane (z=0) and the displacements are shown conceptually in Fig.2.1. The mid-plane strains are:

$$\begin{aligned}
\varepsilon_x^0 &= \frac{\partial u_0}{\partial x} \\
\varepsilon_y^0 &= \frac{\partial v_0}{\partial y} \\
\gamma_{xy}^0 &= \frac{\partial u_0}{\partial y} + \frac{\partial v_0}{\partial x}
\end{aligned} \tag{2.2}$$

Defining the mid-plane strains ε^0 and the plate curvatures κ as in (2.2) and (2.3):

$$\begin{aligned}
\kappa_x &= -\frac{\partial^2 w_0}{\partial x^2} \\
\kappa_y &= -\frac{\partial^2 w_0}{\partial y^2} \\
\kappa_{xy} &= -2\frac{\partial^2 w_0}{\partial x \partial y}
\end{aligned} \tag{2.3}$$

it is possible to rewrite the strain at any point z within the laminate, and subsequently evaluate the stress in the k-th layer using its transformed reduced stiffness matrix $[\bar{Q}]_k$:

$$\begin{bmatrix} \varepsilon_x \\ \varepsilon_y \\ \gamma_{xy} \end{bmatrix} = \begin{bmatrix} \varepsilon_x^0 \\ \varepsilon_y^0 \\ \gamma_{xy}^0 \end{bmatrix} + z \begin{bmatrix} \kappa_x \\ \kappa_y \\ \kappa_{xy} \end{bmatrix} \tag{2.4}$$

$$\begin{Bmatrix} \sigma_x \\ \sigma_y \\ \tau_{xy} \end{Bmatrix}_k = [\bar{Q}]_k \begin{Bmatrix} \varepsilon_x \\ \varepsilon_y \\ \gamma_{xy} \end{Bmatrix} = [\bar{Q}]_k \begin{Bmatrix} \varepsilon_x^0 \\ \varepsilon_y^0 \\ \gamma_{xy}^0 \end{Bmatrix} + z[\bar{Q}]_k \begin{Bmatrix} \kappa_x \\ \kappa_y \\ \kappa_{xy} \end{Bmatrix} \tag{2.5}$$

Where $[\bar{Q}]_k = \begin{bmatrix} \bar{Q}_{xx} & \bar{Q}_{xy} & \bar{Q}_{xs} \\ \bar{Q}_{xy} & \bar{Q}_{yy} & \bar{Q}_{ys} \\ \bar{Q}_{xs} & \bar{Q}_{ys} & \bar{Q}_{ss} \end{bmatrix}_k$ is the transformed reduced stiffness matrix of the k-th layer in the global coordinate system.

What needs to be observed is that the strains vary linearly through the thickness of the entire laminate. Conversely, the stresses also vary linearly within each ply but exhibit discontinuities at the interfaces between adjacent plies (due to different $[\bar{Q}]_k$), as shown in Fig.2.2. A large discontinuity in stresses between plies can promote delamination. This is why laminate design often seeks to avoid abrupt changes in ply orientation, such as placing 0° and 90° plies adjacent to each other, sometimes favoring intermediate angles like ±45°.

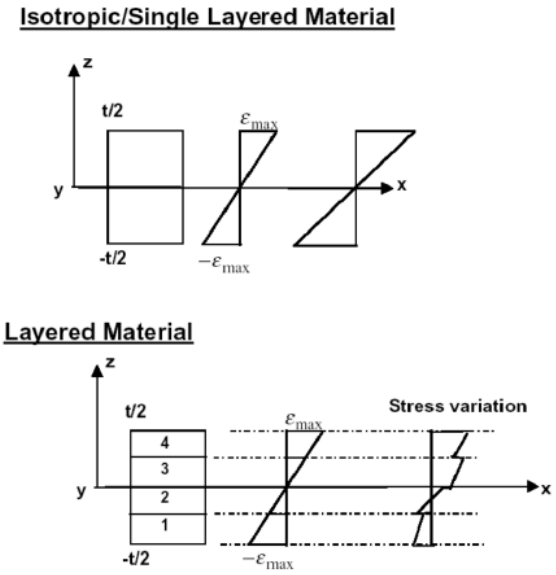

Figure 2.2 Variation of strain (linear) and stress (piecewise linear) through the thickness.

Using the relationship between stresses and the in-plane stress resultants (forces per unit length N) and moment resultants (moments per unit length M):

$$\begin{Bmatrix} N_x \\ N_y \\ N_{xy} \end{Bmatrix} = \sum_{k=1}^{n} \int_{h_{k-1}}^{h_k} \begin{Bmatrix} \sigma_x \\ \sigma_y \\ \tau_{xy} \end{Bmatrix}_k dz \tag{2.6}$$

$$\begin{Bmatrix} M_x \\ M_y \\ M_{xy} \end{Bmatrix} = \sum_{k=1}^{n} \int_{h_{k-1}}^{h_k} \begin{Bmatrix} \sigma_x \\ \sigma_y \\ \tau_{xy} \end{Bmatrix}_k z dz \tag{2.7}$$

where n is the number of plies, and h_k, h_{k-1} are the z-coordinates of the top and bottom surfaces of the k-th ply relative to the laminate mid-plane. Substituting (2.5) into (2.6) and (2.7) and integrating, it is possible to derive the constitutive relationship for the

laminate relating forces/moments to mid-plane strains/curvatures:

$$\begin{Bmatrix} N_x \\ N_y \\ N_{xy} \\ M_x \\ M_y \\ M_{xy} \end{Bmatrix} = \begin{bmatrix} A_{11} & A_{12} & A_{16} & B_{11} & B_{12} & B_{16} \\ A_{12} & A_{22} & A_{26} & B_{12} & B_{22} & B_{26} \\ A_{16} & A_{26} & A_{66} & B_{16} & B_{26} & B_{66} \\ B_{11} & B_{12} & B_{16} & D_{11} & D_{12} & D_{16} \\ B_{12} & B_{22} & B_{26} & D_{12} & D_{22} & D_{26} \\ B_{16} & B_{26} & B_{66} & D_{16} & D_{26} & D_{66} \end{bmatrix} \begin{Bmatrix} \varepsilon_x^0 \\ \varepsilon_y^0 \\ \gamma_{xy}^0 \\ \kappa_x \\ \kappa_y \\ \kappa_{xy} \end{Bmatrix} \tag{2.8}$$

Where: Matrix [A] is the extensional stiffness matrix, relating in-plane forces to in-plane strains.

Matrix [B] is the coupling stiffness matrix, linking in-plane forces to bending/twisting curvatures and, conversely, moments to in-plane strains (extension-bending coupling). If all terms in the [B] matrix were zero (e.g., for symmetric laminates), the in-plane and bending behaviors would be decoupled.

Matrix [D] is the bending stiffness matrix, relating moments to the curvatures required to produce them.

These matrices ([A], [B], [D]) are calculated as follows:

$$\begin{aligned} A_{ij} &= \sum_{k=1}^{n} (\bar{Q}_{ij})_k (h_k - h_{k-1}) \\ B_{ij} &= \frac{1}{2} \sum_{k=1}^{n} (\bar{Q}_{ij})_k (h_k^2 - h_{k-1}^2) \\ D_{ij} &= \frac{1}{3} \sum_{k=1}^{n} (\bar{Q}_{ij})_k (h_k^3 - h_{k-1}^3) \end{aligned} \tag{2.9}$$

for i, j = 1, 2, 6.

2.3 Example Calculation of A, B, D Matrices

A portion of a MATLAB code is presented, used to study a laminate made of Graphite/Epoxy BMS 8-212 Type II Class 1 composite material, whose properties were shown in Table 1.1 in Chapter 1.

Property	Value
E_1	125 GPa
E_2	12.5 GPa
G_{12}	6.89 GPa
ν_{12}	0.38
ν_{21}	0.038

Table 2.1 Material Properties (Same as Table 1.1)

The code snippet allows evaluating the A, B, D matrices once the lamination sequence

(stacking sequence) is assigned. Some interesting sequences are analyzed with this code. The results are compared with results obtained using the Elamx2 software.

For the sequence

$$[90°/45°/-45°/0°]_{3s}$$

the matrix obtained is shown in Fig.2.3-2.4. The analyzed laminate is a symmetric laminate: symmetric laminates are those in which for every ply at a distance +z from the mid-plane, there exists an identical ply (same material, thickness, and orientation) at distance -z. It is observed from the analysis that for symmetric laminates, the coupling matrix [B] has all zero elements ($B_{ij} = 0$): there is no bending-extension coupling. The load-deformation relationship simplifies into two decoupled sets:

$$\begin{Bmatrix} N_x \\ N_y \\ N_{xy} \end{Bmatrix} = \begin{bmatrix} A_{11} & A_{12} & A_{16} \\ A_{12} & A_{22} & A_{26} \\ A_{16} & A_{26} & A_{66} \end{bmatrix} \begin{Bmatrix} \varepsilon_x^0 \\ \varepsilon_y^0 \\ \gamma_{xy}^0 \end{Bmatrix}$$
$$\begin{Bmatrix} M_x \\ M_y \\ M_{xy} \end{Bmatrix} = \begin{bmatrix} D_{11} & D_{12} & D_{16} \\ D_{12} & D_{22} & D_{26} \\ D_{16} & D_{26} & D_{66} \end{bmatrix} \begin{Bmatrix} \kappa_x \\ \kappa_y \\ \kappa_{xy} \end{Bmatrix} \tag{2.10}$$

ABBD

6x6 double

	1	2	3	4	5	6
1	2.0508e+08	6.3392e+07	-5.5336e-09	-2.7285e-12	1.3642e-12	9.3739e-14
2	6.3392e+07	2.0508e+08	1.9254e-09	1.3642e-12	0	-1.0418e-13
3	-5.5336e-09	1.9254e-09	7.0846e+07	9.3739e-14	-1.0418e-13	-2.0464e-12
4	-2.7285e-12	1.3642e-12	9.3739e-14	180.9200	67.4279	6.9345
5	1.3642e-12	0	-1.0418e-13	67.4279	264.1341	6.9345
6	9.3739e-14	-1.0418e-13	-2.0464e-12	6.9345	6.9345	75.4777

Figure 2.3 ABD Matrix for symmetric laminate $[90/45/-45/0]_{3s}$ (MATLAB, values in N/m for A, N for B, N·m for D)

ABD-Matrix

205084.3	63392.5	0.0	-0.0	-0.0	-0.0
63392.5	205084.3	0.0	-0.0	-0.0	0.0
0.0	0.0	70845.9	-0.0	0.0	-0.0
-0.0	-0.0	-0.0	180920.0	67427.9	6934.5
-0.0	-0.0	0.0	67427.9	264134.1	6934.5
-0.0	0.0	-0.0	6934.5	6934.5	75477.7

Figure 2.4 ABD Matrix for symmetric laminate $[90/45/-45/0]_{3s}$ with Elamx2 (values likely in N/mm for A, N for B, N·mm for D)

For the sequence

$$[90°/45°/-45°/0°]_{3a}$$

(assuming 'a' means anti-symmetric) the matrix obtained is shown in Fig.2.5-2.6. The analyzed laminate is an anti-symmetric laminate: anti-symmetric laminates are those where for every ply at +z with orientation θ, there is an identical ply (material, thickness) at -z with orientation $-\theta$. It is observed from the analysis that for anti-symmetric laminates, the bending-twisting coupling terms D_{16} and D_{26} are null. (Note: Depending on the specific definition of anti-symmetric, other terms like $A_{16}, A_{26}, B_{11}, B_{12}, B_{22}, B_{66}$ might also be zero). It is also observed that both analyzed laminates (the symmetric one and this one, if the definition implies balance) are balanced: for every ply with orientation θ, there is always another ply (at any position) with orientation $-\theta$. For balanced laminates, the extensional shear coupling terms A_{16} and A_{26} are null, meaning there is no coupling between normal forces (N_x, N_y) and shear strain (γ^0_{xy}), as observed in the results.

ABBD

6x6 double

	1	2	3	4	5	6
1	2.0508e+08	6.3392e+07	0	0	1.3642e-12	-3.8525e+03
2	6.3392e+07	2.0508e+08	0	1.3642e-12	9.0949e-13	-3.8525e+03
3	0	0	7.0846e+07	-3.8525e+03	-3.8525e+03	-2.0464e-12
4	0	1.3642e-12	-3.8525e+03	264.1341	67.4279	0
5	1.3642e-12	9.0949e-13	-3.8525e+03	67.4279	180.9200	0
6	-3.8525e+03	-3.8525e+03	-2.0464e-12	0	0	75.4777

Figure 2.5 ABD Matrix for anti-symmetric (?) laminate $[90/45/-45/0]_{3a}$ (MATLAB, units as Fig 2.3)

ABD-Matrix

205084.3	63392.5	0.0	-0.0	-0.0	3852.5
63392.5	205084.3	0.0	-0.0	-0.0	3852.5
0.0	0.0	70845.9	3852.5	3852.5	-0.0
-0.0	-0.0	3852.5	180920.0	67427.9	0.0
-0.0	-0.0	3852.5	67427.9	264134.1	0.0
3852.5	3852.5	-0.0	0.0	0.0	75477.7

Figure 2.6 ABD Matrix for anti-symmetric (?) laminate $[90/45/-45/0]_{3a}$ with Elamx2 (units as Fig 2.4)

Other laminates with special properties include Cross-ply laminates, which consist only of plies oriented at 0° and 90°. An example is the laminate with the sequence:

$$[0°/90°]_{12s}$$

whose ABD matrix is shown in Fig.2.7-2.8. For this specific symmetric cross-ply laminate, it is observed that the coupling terms A_{16}, A_{26}, B_{ij} (all B terms are zero due to symmetry), and D_{16}, D_{26} are null. Additionally, if the number of 0° and 90° plies is equal, we might expect $A_{11} \approx A_{22}$ and $D_{11} \approx D_{22}$. (The original text observation $A_{x,x} = A_{y,y}$, $B_{x,x} = -B_{y,y}$, $D_{x,x} = D_{y,y}$ seems specific and might depend on the exact layup and reference frame).

Let's check the figure: $A_{11} = A_{22}$, $D_{11} = D_{22}$ and $B_{ij} = 0$. $A_{16} = A_{26} = D_{16} = D_{26} = 0$. This confirms special orthotropy.

ABBD

6x6 double

	1	2	3	4	5	6
1	2.5113e+08	1.7351e+07	6.5210e-10	-1.5410e+04	6.8212e-13	4.8908e-14
2	1.7351e+07	2.5113e+08	1.1929e-08	6.8212e-13	1.5410e+04	8.9468e-13
3	6.5210e-10	1.1929e-08	24804000	4.8908e-14	8.9468e-13	1.1369e-12
4	-1.5410e+04	6.8212e-13	4.8908e-14	271.2164	18.7386	7.0427e-16
5	6.8212e-13	1.5410e+04	8.9468e-13	18.7386	271.2164	1.2883e-14
6	4.8908e-14	8.9468e-13	1.1369e-12	7.0427e-16	1.2883e-14	26.7883

Figure 2.7 ABD Matrix for Cross-Ply laminate $[0/90]_{12s}$ (MATLAB, units as Fig 2.3)

ABD-Matrix

251126.3	17350.5	0.0	15410.0	-0.0	-0.0
17350.5	251126.3	0.0	-0.0	-15410.0	-0.0
0.0	0.0	24804.0	-0.0	-0.0	-0.0
15410.0	-0.0	-0.0	271216.4	18738.6	0.0
-0.0	-15410.0	-0.0	18738.6	271216.4	0.0
-0.0	-0.0	-0.0	0.0	0.0	26788.3

Figure 2.8 ABD Matrix for Cross-Ply laminate $[0/90]_{12s}$ with Elamx2 (units as Fig 2.4)

Listing 2.1 MATLAB code snippet for calculating A, B, D matrices.

```
%% sequenza di laminazione
seq_theta1 = [0 45 -45 90 0 45 -45 90 0 +45 -45 90];
seq_theta = [seq_theta1, fliplr(seq_theta1)];
seq_theta_rad = convang(seq_theta,'deg','rad');

N = length(seq_theta_rad);
z_vec = t * linspace((-N/2),(N/2),N+1);
z_mean= z_vec(2:end)-t/2;
%% costruzione matrici A, B, D
A = zeros(3);
B = zeros(3);
D = zeros(3);

for i=1:N
    A = A + Q_glob(seq_theta_rad(i)) * (z_vec(i+1) - z_vec(i));
    B = B + Q_glob(seq_theta_rad(i)) * ((z_vec(i+1))^2 - (z_vec(i))^2)/2;
    D = D + Q_glob(seq_theta_rad(i)) * ((z_vec(i+1))^3 - (z_vec(i))^3)/3;
end
ABBD = [A B; B D]
```

2.4 Example of Carpet Plot

In the previous section, it was illustrated how to calculate the A, B, D matrices of the laminate, which allow constructing the relationship between loads (N, M) and deformations (ε^0, κ). Once these matrices are constructed, specifically the extensional stiffness matrix [A], it is possible to derive the effective in-plane elastic moduli and Poisson's ratios of the laminate using the following relationships:

$$\begin{aligned} \overline{E}_x &= \frac{1}{h \cdot a_{11}} \\ \overline{E}_y &= \frac{1}{h \cdot a_{22}} \\ \overline{G}_{xy} &= \frac{1}{h \cdot a_{66}} \\ \overline{\nu}_{xy} &= -\frac{a_{12}}{a_{11}} \\ \overline{\nu}_{yx} &= -\frac{a_{12}}{a_{22}} \end{aligned} \tag{2.11}$$

where $[a] = [A]^{-1}$ is the inverse of the extensional stiffness matrix (the in-plane compliance matrix), h is the total laminate thickness, and a_{ij} are the components of the $[a]$ matrix. (The original text used ta_{xx}, etc. Assuming t meant thickness h, and a_{xx} meant a_{11}).

A MATLAB code is presented below that allows constructing Carpet Plots for laminates, shown in Fig.2.9, Fig.2.10, Fig.2.11. The plots show how the effective properties of the laminate vary as the percentages of plies oriented at 0°, 90°, and ±45° change (assuming a standard family, e.g., $0_x/\pm 45_y/90_z$ where $x + y + z = 100\%$). These graphs can be very useful in the laminate design phase to choose the most appropriate stacking sequence. However, carpet plots based solely on Classical Lamination Theory cannot typically be used directly for certification purposes. This is because certifying authorities often require that allowable properties used in design (which might be derived from such plots) are

validated or derived from experimental testing.

Listing 2.2 MATLAB code snippet for generating Carpet Plots.

```
%% DIVERSE SEQUENZE di laminazione
%% valuto effetto variazione di % di +- 45   e 90
%% consideriamo solo laminato simmetrico (non tengo conto particolare posizionamento)
%% fisso numero lamine a 20
N_lam = 20;
seq_0 = zeros(1,N_lam);
seq_pm45 = [45, -45];
seq_pm45 = [seq_pm45, seq_pm45, seq_pm45, seq_pm45, seq_pm45, seq_pm45 ...
            seq_pm45, seq_pm45, seq_pm45, seq_pm45];
seq_pm45 = convang(seq_pm45,'deg','rad');
seq_90 = convang(90,'deg','rad')*ones(1,N_lam);
N_perc = N_lam/2;
perc_vec=linspace(0,100,N_perc+1);
E_x_mat = nan(N_perc);
G_xy_mat = nan(N_perc);
nu_xy_mat = nan(N_perc);
E_x_1vec = nan(N_perc,1);
G_xy_1vec = nan(N_perc,1);
nu_xy_1vec = nan(N_perc,1);
E_x_2vec = nan(N_perc,1);
G_xy_2vec = nan(N_perc,1);
nu_xy_2vec = nan(N_perc,1);


for i=1:(N_perc-1)
    for j=1:(N_perc-i)
        %% al variare di i varia la percentuale di lamine a 0
        %% al variare di j varia la percentuale di +-45
        if (i+j)<N_perc
            seq_theta=[seq_0(1:(2*i)),seq_pm45(1:2*j), seq_90(1:(N_lam -2*(i+j)))];
        elseif (i<N_perc) && (i+j==N_perc)
                seq_theta=[seq_0(1:(2*i)),seq_pm45(1:2*j)];
        end
        seq_theta_rad = [seq_theta, fliplr(seq_theta)];


        N = length(seq_theta_rad);
        z_vec = t * linspace((-N/2),(N/2),N+1);
        %% costruzione matrici A, B, D
        A = zeros(3);
        B = zeros(3);
        D = zeros(3);
        for k=1:N
            A = A + Q_glob(seq_theta_rad(k)) * (z_vec(k+1) - z_vec(k));
            B = B + Q_glob(seq_theta_rad(k)) * ((z_vec(k+1))^2 - (z_vec(k))^2)/2;
            D = D + Q_glob(seq_theta_rad(k)) * ((z_vec(k+1))^3 - (z_vec(k))^3)/3;
        end
        ABBD = [A B; B D];
```

```
        ABBD_inv = inv(ABBD);
        %% moduli elastici effettivi
        E_x = 1/(ABBD_inv(1,1)*t*N*6.89);
        G_xy = 1/(ABBD_inv(3,3)*t*N);
        ni_xy = - ABBD_inv(1,2) / ABBD_inv(1,1);
        E_x_mat(i,j) = E_x;
        G_xy_mat(i,j) = G_xy;
        nu_xy_mat(i,j) = ni_xy;
        %% moduli di bending
        E_bx = 12/(ABBD_inv(4,4)*(t*N)^3);
        E_by = 12/(ABBD_inv(5,5)*(t*N)^3);
    end
end
```

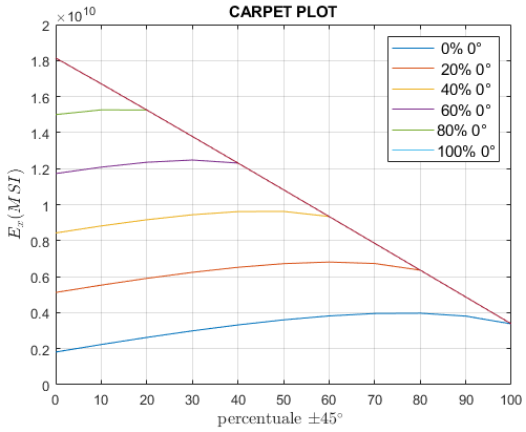

Figure 2.9 Carpet plot for effective modulus $\overline{E}_x$ vs. ply percentages.

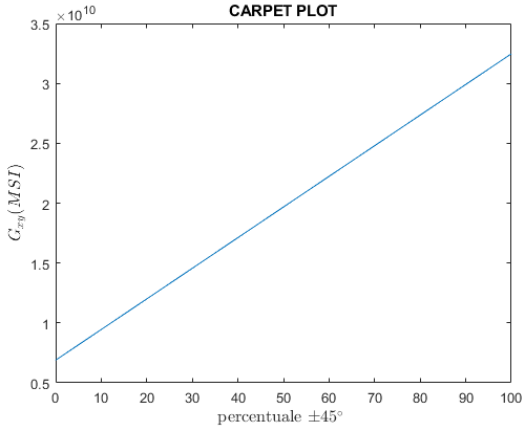

Figure 2.10 Carpet plot for effective shear modulus $\overline{G}_{xy}$ vs. ply percentages.

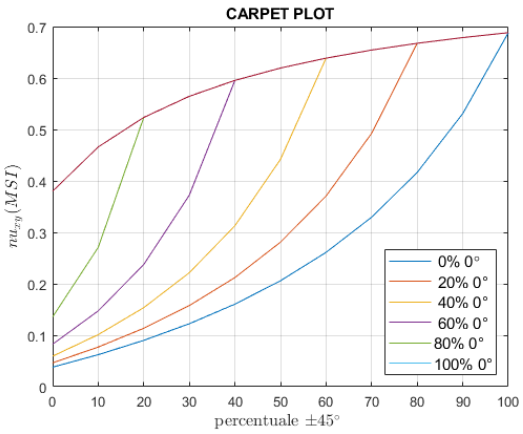

Figure 2.11 Carpet plot for effective Poisson's ratio $\overline{\nu}_{xy}$ vs. ply percentages.

2.5 Failure Criteria, Design of a Composite Fuselage Panel

Evaluating the ability of a composite material layer (ply) within a laminate to withstand operational stresses and strains involves complex analysis, considering various failure criteria. Among the most important criteria used are:

- Maximum Stress Criterion: This criterion states that failure occurs when a stress component $(\sigma_1, \sigma_2, \tau_{12})$ in the ply's local material coordinates reaches the corresponding ultimate strength of the material (X_t, X_c, Y_t, Y_c, S). Failure is predicted if any of these conditions are met: $\sigma_1 > X_t$ or $\sigma_1 < -X_c$; $\sigma_2 > Y_t$ or $\sigma_2 < -Y_c$; $|\tau_{12}| > S$.

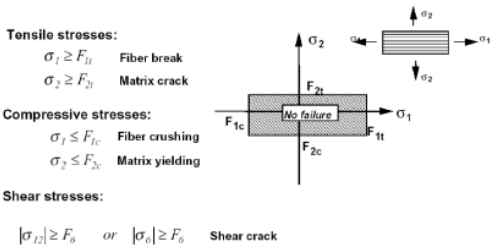

Figure 2.12 Maximum Stress Criterion failure envelope (schematic).

- Maximum Strain Criterion: Similar to the maximum stress theory, but failure is predicted when a strain component $(\epsilon_1, \epsilon_2, \gamma_{12})$ in the local coordinates reaches the ultimate strain limit of the material $(\epsilon^u_{1t}, \epsilon^u_{1c}, \epsilon^u_{2t}, \epsilon^u_{2c}, \gamma^u_{12})$.
- Tsai-Hill and Tsai-Wu Criteria: These are interactive (quadratic) criteria that consider the combined effect of multiple stress components acting simultaneously. They define a failure surface in stress space. Tsai-Wu is generally more flexible as it includes linear terms and can distinguish between tensile and compressive strengths more easily.

In practice, to determine if a composite laminate can withstand a given load combination, the following procedure is often used (ply-by-ply analysis):

- Calculate the global strains (ε^0, κ) for the applied loads (N, M) using the laminate's ABD matrix.

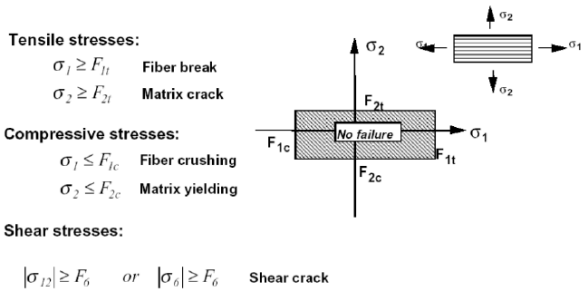

Figure 2.13 Maximum Strain Criterion failure envelope (schematic).

Figure 2.14 Tsai-Hill Criterion failure envelope (schematic).

- Calculate the local strains ($\epsilon_1, \epsilon_2, \gamma_{12}$) in each ply using the strain transformation and Eq. (2.4).
- Calculate the local stresses ($\sigma_1, \sigma_2, \tau_{12}$) in each ply using its local stiffness matrix [Q] or from global stresses using stress transformation.
- Apply multiple failure criteria (e.g., Max Stress, Max Strain, Tsai-Hill, Tsai-Wu) to the calculated local stresses/strains for each ply.
- Calculate the Failure Index (F.I.) or Reserve Factor (R.F. = 1/F.I.) for each criterion and each ply. Failure is predicted if F.I. $\geq$ 1 (or R.F. $\leq$ 1). The Margin of Safety (M.S.) is often defined as M.S. = R.F. - 1 (or sometimes M.S. = 1/F.I. - 1).
- The critical ply and critical criterion are those resulting in the lowest R.F. (or highest F.I., or lowest M.S.).

Therefore, generally, multiple failure criteria are applied because no single criterion is universally the most conservative or accurate for all materials and loading conditions, as illustrated schematically in Fig.2.15.

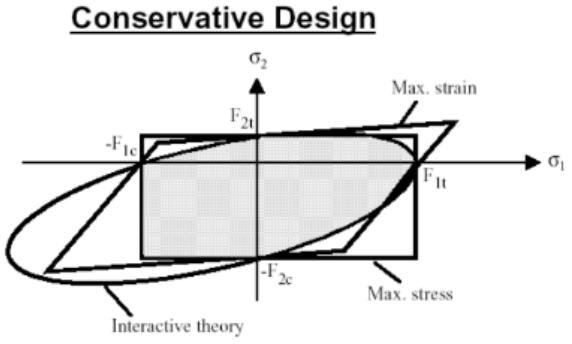

Figure 2.15 Comparison of different failure criteria envelopes, showing none is universally most conservative.

During design, it must be considered that composite materials are characterized by numerous issues and critical phenomena that are difficult to model accurately. In

some cases, even if accurate models describing such phenomena have been developed, it is complicated to obtain the necessary material parameters experimentally. For this reason, aerospace regulations for designing with composite materials are quite stringent, particularly establishing significantly reduced design limit and ultimate allowables (knock-down factors). Among the phenomena contributing to these reductions are:

- Potential for delamination due to high interlaminar stresses, especially near edges or discontinuities, or due to significant stress jumps between plies (e.g., adjacent $0°/90°$). This often leads to designs with smoother orientation changes, using high percentages of $\pm 45°$ plies.
- Reduction in strength due to residual stresses arising from thermal variations during curing or environmental effects (temperature, humidity). Tests are often required under adverse environmental conditions, such as "hot-wet".
- Reduction in strength due to manufacturing defects (e.g., voids, fiber waviness).
- Susceptibility to impact damage, which can cause significant internal delamination with little visible surface indication (Barely Visible Impact Damage - BVID). This contrasts with metals like aluminum where damage is often visually inspectable. This is also a key reason why fatigue and damage tolerance assessments for composites differ from traditional materials: composite structures are often designed assuming the presence of initial damage (e.g., impact damage of a certain energy level) and must demonstrate that this damage does not grow catastrophically during the service life (damage tolerance philosophy). Fatigue testing might involve pre-damaging specimens.
- Presence of stress concentrations (e.g., around holes) significantly reduces the load-carrying capacity. Laminates with a high percentage of $\pm 45°$ plies can sometimes mitigate this strength reduction compared to highly orthotropic layups.

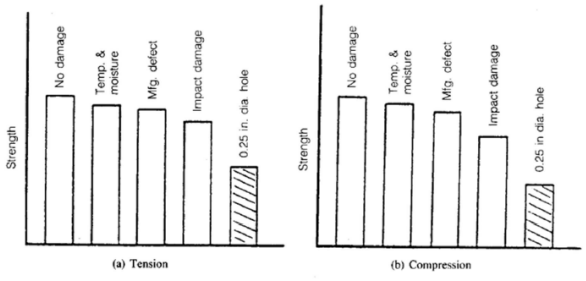

Fig. 7.1.11 Factors Affecting Design Strength

Figure 2.16 Factors contributing to the reduction of material design allowables (knock-down factors).

2.5.1 Fuselage Panel Example

In this final part of the chapter, we examine some design considerations for a composite panel, taking a specific case study. For this study, a fuselage panel made of Graphite/Epoxy BMS 8-212 Type II Class 1 composite material (properties in Table 2.1) is considered,

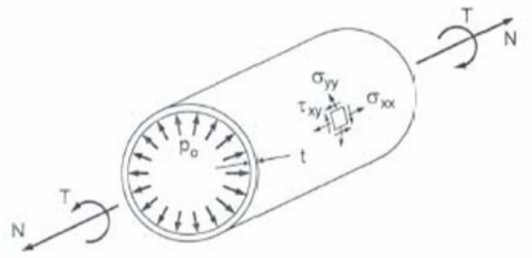

Figure 2.17 Fuselage Panel under Pressure and Torsion.

subjected to internal pressurization and a torsional moment, as depicted conceptually in Fig.2.17.

The chosen load values and geometry are presented in Table 2.2.

ΔP (Pressure differential)	0.180 MPa
M_T (Torsional moment)	4.5×10^6 Nm
Required $M.S.$ (Margin of Safety)	0.5
R (Fuselage radius)	1.5 m
t_{ply} (Single ply thickness)	0.15 mm

Table 2.2 Loads and Geometric Data

Given the loads and geometry, it is possible to derive the membrane stresses (σ) and the corresponding in-plane load resultants per unit length (N) using simple static equilibrium considerations for a thin-walled cylinder and Bredt's formula for torsion:

$$\begin{cases} \sigma_L = \frac{\Delta P \cdot R}{2 \cdot t_{total}} & \text{(Axial stress)} \\ \sigma_H = \frac{\Delta P \cdot R}{t_{total}} & \text{(Hoop stress)} \\ \tau_{xy} = \frac{M_T}{2\pi R^2 t_{total}} & \text{(Shear stress)} \end{cases} \tag{2.12}$$

$$\begin{cases} N_x = \sigma_L \cdot t_{total} = \frac{\Delta P \cdot R}{2} & \text{(Axial load/length)} \\ N_y = \sigma_H \cdot t_{total} = \Delta P \cdot R & \text{(Hoop load/length)} \\ N_{xy} = \tau_{xy} \cdot t_{total} = \frac{M_T}{2\pi R^2} & \text{(Shear load/length)} \end{cases} \tag{2.13}$$

Where t_{total} is the total laminate thickness. Note the correspondence N_x with longitudinal direction (σ_L) and N_y with hoop direction (σ_H).

We follow this design procedure: First step is to choose the percentages of plies at 0°, ±45°, and 90° (relative to the fuselage axis, typically 0°). When predominant loads act in a specific direction (e.g., hoop stress from pressure), increasing the percentage of plies aligned with that direction (90°) is beneficial. However, the increase in allowable load may not be linear with the percentage increase. Also, ±45° plies are very efficient for carrying shear loads (from torsion) and contribute significantly to damage tolerance (e.g., around holes, impacts). For these reasons, a balanced approach often involves a significant percentage of ±45° plies. The proposed code considers a quasi-isotropic

laminate as a starting point:

$$[90^\circ/\pm 45^\circ/0^\circ]_{ns}$$

where 'n' determines the total number of plies ($N_{plies} = 4 \times n \times 2 = 8n$) and 's' denotes symmetry.

Second step is to estimate the required number of plies (or total thickness $t_{total} = N_{plies} \times t_{ply}$). This can be done by using Carpet Plots of allowable loads (like those in Fig.2.18, Fig.2.19, Fig.2.20) for the chosen family of layups (e.g., varying percentages of $0/\pm 45/90$). From these plots, one can estimate the ultimate load carrying capability ($N_x^{ult}, N_y^{ult}, N_{xy}^{ult}$) for a candidate layup. The required thickness must ensure that the applied loads multiplied by the load factor (typically 1.5 for ultimate load) are less than the allowable loads, satisfying the required Margin of Safety (M.S. = Allowable Load / (Applied Load * Load Factor) - 1 ≥ Required M.S.).

Third step is to perform a detailed ply-by-ply failure analysis for the selected laminate (stacking sequence and thickness) under the design loads. Calculate the Failure Indices (F.I.) or Reserve Factors (R.F.) for each ply using multiple criteria and verify that the minimum Margin of Safety meets the requirement (M.S. ≥ 0.5).

Finally, the procedure can be iterated by slightly adjusting the stacking sequence (percentages or ply order) or thickness to optimize for minimum weight while satisfying all requirements.

The MATLAB code used for this study is presented below.

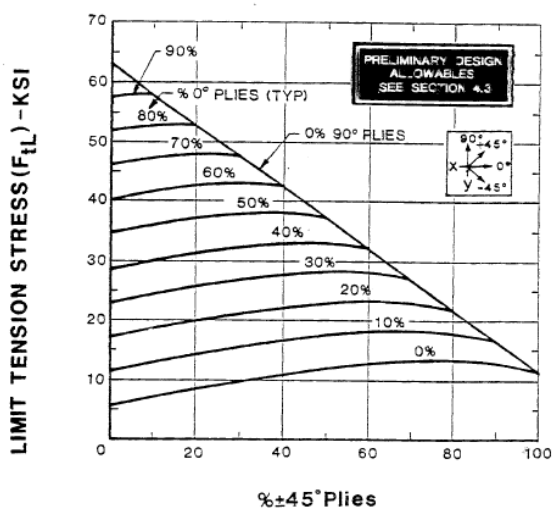

Figure 2.18 Carpet Plot Example: Ultimate Tensile Load Allowable (N_x^t or N_y^t).

Listing 2.3 MATLAB code for fuselage panel analysis.

```
clc;
clear;
close all;

%% moduli elastici della lamina e propriet  gemometriche
E_1 = 125e9; %(Pa)
E_2 = 12.5e9; %(Pa)
ni_12 = 0.38;
G_12 = 6.89e9; %(Pa)
t = 0.15e-3; %(m)
```

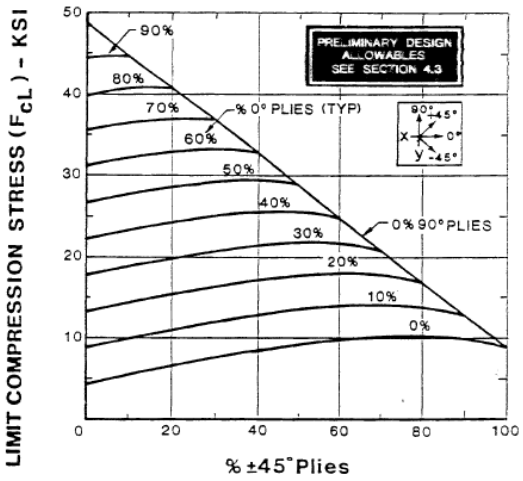

Figure 2.19 Carpet Plot Example: Ultimate Compressive Load Allowable (N_x^c or N_y^c).

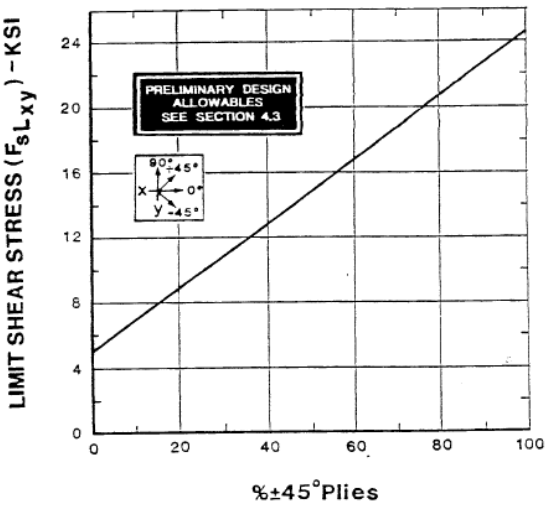

Figure 2.20 Carpet Plot Example: Ultimate Shear Load Allowable (N_{xy}^{ult}).

```
11
12 %% carichi esterni apllicati
13 Delta_P = 0.18e6; %(Pa) carico di pressurizzazione
14 M_T = 2.5e6; %(Nm)
15 R = 2; %(m) raggio di fusoliera
16 M_S = 0.5; %(m) Margine di sicurezza assegnato
17 fat_ampl = 1+M_S; % per il calcolo
18 %valuto carichi per unit  di lunghezza
19 M_x = 0; %(Nm)
20 M_y = 0; %(Nm)
21 M_xy = 0;%(Nm)
22 N_x = Delta_P * R/2 ; %(N/m)
23 N_y = Delta_P * R; %(N/m)
24 N_xy = M_T/(2*pi*R^2); %(N/m)
25
26 N_M_ul = [N_x N_y N_xy M_x M_y M_xy];
27
28
29 %% sequenza di laminazione
30 %% scelgo un laminato simmetrico e trasversalmente isotropo
```

```
seq_theta1 = [0 45 -45 90];

% Definisco carichi ultimi laminato usando carpet plot nota la sequenza
sigma_xLT = 172e6; %(Pa)
sigma_yLT = 172e6; %(Pa)
tauxy_L = 96e6; %(Pa)

%% calcolo spessore e quindi numero di lamine
N_xt = ceil(N_x*fat_ampl/(sigma_xLT*8*t));
N_yt = ceil(N_y*fat_ampl/(sigma_yLT*8*t));
N_st = ceil(N_xy*fat_ampl/(tauxy_L*8*t));
M = max([N_xt, N_yt, N_st]);
seq_theta2=seq_theta1;
for i=1:M-1
    seq_theta2=[seq_theta2, seq_theta1];
end
seq_theta = [seq_theta2, fliplr(seq_theta2)];
seq_theta_rad = convang(seq_theta,'deg','rad');
N = length(seq_theta_rad);
fprintf('Il numero di lamine    %f \n',N);

%% matrice Q
Q_11 = E_1/(1-(E_2/E_1)*(ni_12)^2);
Q_12 = ni_12*E_2/(1-(E_2/E_1)*(ni_12)^2);
Q_22 = E_2/(1-(E_2/E_1)*(ni_12)^2);
Q_66 = G_12;

Q=[Q_11 Q_12 0;
    Q_12 Q_22 0;
    0 0 Q_66];

%% calcolo matrici di rotazione
T_sigma = @(theta) [(cos(theta))^2  (sin(theta))^2  -2*cos(theta)*sin(
   theta);
    (sin(theta))^2  (cos(theta))^2  2*cos(theta)*sin(theta);
    cos(theta)*sin(theta)  -cos(theta)*sin(theta)  (cos(theta))^2-(sin(
   theta))^2];

T_eps = @(theta) [(cos(theta))^2  (sin(theta))^2  -cos(theta)*sin(theta);
    (sin(theta))^2  (cos(theta))^2  cos(theta)*sin(theta);
    2*cos(theta)*sin(theta)  -2*cos(theta)*sin(theta)  (cos(theta))^2-(
   sin(theta))^2];

%% calcolo matrici Q nel riferimento globale
Q_glob = @(theta) (T_sigma(theta) * Q) / T_eps(theta);

%% costruzione matrici A, B, D
z_vec = t * linspace((-N/2),(N/2),N+1);
z_mean= z_vec(2:end)-t/2;
A = zeros(3);
B = zeros(3);
D = zeros(3);

for i=1:N
    A = A + Q_glob(seq_theta_rad(i)) * (z_vec(i+1) - z_vec(i));
    B = B + Q_glob(seq_theta_rad(i)) * ((z_vec(i+1))^2 - (z_vec(i))^2)/2;
```

```
    D = D + Q_glob(seq_theta_rad(i)) * ((z_vec(i+1))^3 - (z_vec(i))^3)/3;
end
ABBD = [A B; B D];
ABBD_inv = inv(ABBD);

%% moduli elastici effettivi
E_x = 1/(ABBD_inv(1,1)*t*N);
E_y = 1/(ABBD_inv(2,2)*t*N);
G_xy = 1/(ABBD_inv(3,3)*t*N);
ni_xy = - ABBD_inv(1,2) / ABBD_inv(1,1);

%% moduli di bending
E_bx = 12/(ABBD_inv(4,4)*(t*N)^3);
E_by = 12/(ABBD_inv(5,5)*(t*N)^3);


%% calcolo deformazioni
eps_k = ABBD\N_M_ul(:);
eps_mat_glob = zeros(3,N);
sigma_mat_glob = zeros(3,N);
eps_mat_loc = zeros(3,N);
sigma_mat_loc = zeros(3,N);

for i=1:N

    eps_mat_glob(:,i) = eps_k(1:3) + z_mean(i)*eps_k(4:6);
    sigma_mat_glob(:,i) = Q_glob(seq_theta_rad(i))*eps_mat_glob(:,i);

    eps_mat_loc(:,i) = T_eps(seq_theta_rad(i))\eps_mat_glob(:,i);
    sigma_mat_loc(:,i) = T_sigma(seq_theta_rad(i))\sigma_mat_glob(:,i);

end

%% Indici di Failure
%% Definisco carichi ultimi lamina usando carpet plot
%% calcolo margini di stabilit

sigma_1LT = 434e6; %(Pa)
sigma_2LT = 41.4e6; %(Pa)
sigma_1LC = -331e6; %(Pa)
sigma_2LC = -27.6e6; %(Pa)
tau_L = 34.5e6; %(Pa)

eps_1LT =  sigma_1LT / E_1;
eps_2LT =  sigma_2LT / E_2;
eps_1LC =  sigma_1LC / E_1;
eps_2LC =  sigma_2LC / E_2;
gam_L = tau_L / G_12;

Fail_ind= zeros(7,1);
I = zeros(6,1);

MaxStress1 = zeros(1,N);
MaxStress2 = zeros(1,N);
MaxStressS = zeros(1,N);

```

```
MaxStrain1 = zeros(1,N);
MaxStrain2 = zeros(1,N);
MaxStrainS = zeros(1,N);
TH = zeros(1,N);

%% max stress e max strain
for i=1:N

if sigma_mat_loc(1,i)<0
    MaxStress1(i) = sigma_1LC/sigma_mat_loc(1,i);
    % costruisco un termine per applicare Tsai-Hill
    TH(1,i) = (sigma_mat_loc(1,i)*sigma_mat_loc(2,i))/(sigma_1LC^2);
else
    MaxStress1(i) = sigma_1LT/sigma_mat_loc(1,i);
     % costruisco un termine per applicare Tsai-Hill
    TH(1,i) = (sigma_mat_loc(1,i)*sigma_mat_loc(2,i))/(sigma_1LT^2);
end


if sigma_mat_loc(2,i)<0
    MaxStress2(i) = sigma_2LC/sigma_mat_loc(2,i);
else
    MaxStress2(i) = sigma_2LT/sigma_mat_loc(2,i);
end

if eps_mat_loc(1,i)<0
    MaxStrain1(i) = eps_1LC/eps_mat_loc(1,i);
else
    MaxStrain1(i) = eps_1LT/eps_mat_loc(1,i);
end

if eps_mat_loc(2,i)<0
    MaxStrain2(i) = eps_2LC/eps_mat_loc(2,i);
else
    MaxStrain2(i) = eps_2LT/eps_mat_loc(2,i);
end


end

MaxStressS = abs(tau_L./sigma_mat_loc(3,:));
MaxStrainS = abs(gam_L./eps_mat_loc(3,:));

%% Tsai Hill
TsaiHill = (1./(((1./MaxStress1).^2)+((1./MaxStress2).^2)+((1./MaxStressS
   ).^2) - TH)).^(1/2);

%% Tsai-Wu
f1 = (1/(sigma_1LT)) + (1/(sigma_1LC));
f11 = -1/(sigma_1LT*sigma_1LC);
f2 = (1/(sigma_2LT)) + (1/(sigma_2LC));
f22 = -1/(sigma_2LT*sigma_2LC);
f66 = 1/(tau_L^2);
f12 = -(1/2)*((f11*f22)^(1/2));

B =  f1*sigma_mat_loc(1,:) + f2*sigma_mat_loc(2,:);
```

```
A =  f11*(sigma_mat_loc(1,:).^2) + f22*(sigma_mat_loc(2,:).^2) + ...
    f66*(sigma_mat_loc(3,:).^2) + 2*f12*(sigma_mat_loc(1,:).*(
   sigma_mat_loc(2,:)));
C = -1;

TsaiWu = (-B + ((B.^2 - 4*A.*C)).^(1/2))./(2*A);

%% calcolo indice di sicurezza minimo
[Fail_ind(1), I(1)] = min(MaxStress1);
[Fail_ind(2), I(2)] = min(MaxStress2);
[Fail_ind(3), I(3)] = min(MaxStressS);
[Fail_ind(4), I(4)] = min(MaxStrain1);
[Fail_ind(5), I(5)] = min(MaxStrain2);
[Fail_ind(6), I(6)] = min(MaxStrainS);
[Fail_ind(7), I(7)] = min(TsaiHill);
[Fail_ind(8), I(8)] = min(TsaiWu);

%Calcolo Failure index minimo e mostro
[Fail_index,pos]= min (Fail_ind);
fprintf('Indice di failure    %f \n',Fail_index);
strin = ["MaxStress1", "MaxStress2", "MaxStressS", ...
         "MaxStrain1", "MaxStrain2", "MaxStrainS", "TsaiHill", "TsaiWu"];

d=strin(pos);
disp('Si    ottenuto con il criterio di ');
disp(d);
fprintf('nella lamina  %f \n',I(pos));
```

lamina	seq_theta	σx	σy	τxy	εx	εy	γxy
1	0	5.4898e+07	2.2597e+07	1.7413e+07	3.7049e-04	0.0016	0.0025
2	45	1.3837e+08	1.5587e+08	1.3946e+08	3.7049e-04	0.0016	0.0025
3	-45	-5.8747e+06	1.1631e+07	2.4661e+07	3.7049e-04	0.0016	0.0025
4	90	1.2607e+07	2.0990e+08	1.7413e+07	3.7049e-04	0.0016	0.0025
5	0	5.4898e+07	2.2597e+07	1.7413e+07	3.7049e-04	0.0016	0.0025
6	45	1.3837e+08	1.5587e+08	1.3946e+08	3.7049e-04	0.0016	0.0025
7	-45	-5.8747e+06	1.1631e+07	2.4661e+07	3.7049e-04	0.0016	0.0025
8	90	1.2607e+07	2.0990e+08	1.7413e+07	3.7049e-04	0.0016	0.0025
9	0	5.4898e+07	2.2597e+07	1.7413e+07	3.7049e-04	0.0016	0.0025
10	45	1.3837e+08	1.5587e+08	1.3946e+08	3.7049e-04	0.0016	0.0025
11	-45	-5.8747e+06	1.1631e+07	2.4661e+07	3.7049e-04	0.0016	0.0025
12	90	1.2607e+07	2.0990e+08	1.7413e+07	3.7049e-04	0.0016	0.0025
13	90	1.2607e+07	2.0990e+08	1.7413e+07	3.7049e-04	0.0016	0.0025
14	-45	-5.8747e+06	1.1631e+07	2.4661e+07	3.7049e-04	0.0016	0.0025
15	45	1.3837e+08	1.5587e+08	1.3946e+08	3.7049e-04	0.0016	0.0025
16	0	5.4898e+07	2.2597e+07	1.7413e+07	3.7049e-04	0.0016	0.0025
17	90	1.2607e+07	2.0990e+08	1.7413e+07	3.7049e-04	0.0016	0.0025
18	-45	-5.8747e+06	1.1631e+07	2.4661e+07	3.7049e-04	0.0016	0.0025
19	45	1.3837e+08	1.5587e+08	1.3946e+08	3.7049e-04	0.0016	0.0025
20	0	5.4898e+07	2.2597e+07	1.7413e+07	3.7049e-04	0.0016	0.0025
21	90	1.2607e+07	2.0990e+08	1.7413e+07	3.7049e-04	0.0016	0.0025
22	-45	-5.8747e+06	1.1631e+07	2.4661e+07	3.7049e-04	0.0016	0.0025
23	45	1.3837e+08	1.5587e+08	1.3946e+08	3.7049e-04	0.0016	0.0025
24	0	5.4898e+07	2.2597e+07	1.7413e+07	3.7049e-04	0.0016	0.0025

Figure 2.21 Calculated Stresses and Strains in the Global (x-y) Reference Frame.

lamina	seq_theta	σ1	σ2	τ12	ε1	ε2	γ12
1	0	5.4898e+07	2.2597e+07	1.7413e+07	3.7049e-04	0.0016	0.0025
2	45	2.8658e+08	7.6652e+06	8.7528e+06	0.0023	-2.5798e-04	0.0013
3	-45	-2.1783e+07	2.7539e+07	-8.7528e+06	-2.5798e-04	0.0023	-0.0013
4	90	2.0990e+08	1.2607e+07	-1.7413e+07	0.0016	3.7049e-04	-0.0025
5	0	5.4898e+07	2.2597e+07	1.7413e+07	3.7049e-04	0.0016	0.0025
6	45	2.8658e+08	7.6652e+06	8.7528e+06	0.0023	-2.5798e-04	0.0013
7	-45	-2.1783e+07	2.7539e+07	-8.7528e+06	-2.5798e-04	0.0023	-0.0013
8	90	2.0990e+08	1.2607e+07	-1.7413e+07	0.0016	3.7049e-04	-0.0025
9	0	5.4898e+07	2.2597e+07	1.7413e+07	3.7049e-04	0.0016	0.0025
10	45	2.8658e+08	7.6652e+06	8.7528e+06	0.0023	-2.5798e-04	0.0013
11	-45	-2.1783e+07	2.7539e+07	-8.7528e+06	-2.5798e-04	0.0023	-0.0013
12	90	2.0990e+08	1.2607e+07	-1.7413e+07	0.0016	3.7049e-04	-0.0025
13	90	2.0990e+08	1.2607e+07	-1.7413e+07	0.0016	3.7049e-04	-0.0025
14	-45	-2.1783e+07	2.7539e+07	-8.7528e+06	-2.5798e-04	0.0023	-0.0013
15	45	2.8658e+08	7.6652e+06	8.7528e+06	0.0023	-2.5798e-04	0.0013
16	0	5.4898e+07	2.2597e+07	1.7413e+07	3.7049e-04	0.0016	0.0025
17	90	2.0990e+08	1.2607e+07	-1.7413e+07	0.0016	3.7049e-04	-0.0025
18	-45	-2.1783e+07	2.7539e+07	-8.7528e+06	-2.5798e-04	0.0023	-0.0013
19	45	2.8658e+08	7.6652e+06	8.7528e+06	0.0023	-2.5798e-04	0.0013
20	0	5.4898e+07	2.2597e+07	1.7413e+07	3.7049e-04	0.0016	0.0025
21	90	2.0990e+08	1.2607e+07	-1.7413e+07	0.0016	3.7049e-04	-0.0025
22	-45	-2.1783e+07	2.7539e+07	-8.7528e+06	-2.5798e-04	0.0023	-0.0013
23	45	2.8658e+08	7.6652e+06	8.7528e+06	0.0023	-2.5798e-04	0.0013
24	0	5.4898e+07	2.2597e+07	1.7413e+07	3.7049e-04	0.0016	0.0025

Figure 2.22 Calculated Stresses and Strains in the Local (1-2) Reference Frame for each ply.

Local layer results :

No.	zmi		s11	s22	s12	e11	e22	e12	RF
1	1.72500E+00	upper	5.48983E+01	2.25968E+01	1.74132E+01	3.70492E-04	1.64085E-03	2.52732E-03	1.33383E+00
2	1.57500E+00	upper	2.86579E+02	7.66521E+00	8.75280E+00	2.26933E-03	-2.57984E-04	1.27036E-03	1.38276E+00
3	1.42500E+00	upper	-2.17832E+01	2.75389E+01	-8.75280E+00	-2.57984E-04	2.26933E-03	-1.27036E-03	1.39124E+00
4	1.27500E+00	upper	2.09898E+02	1.26073E+01	-1.74132E+01	1.64085E-03	3.70492E-04	-2.52732E-03	1.32763E+00
5	1.12500E+00	upper	5.48983E+01	2.25968E+01	1.74132E+01	3.70492E-04	1.64085E-03	2.52732E-03	1.33383E+00
6	9.75000E-01	upper	2.86579E+02	7.66521E+00	8.75280E+00	2.26933E-03	-2.57984E-04	1.27036E-03	1.38276E+00
7	8.25000E-01	upper	-2.17832E+01	2.75389E+01	-8.75280E+00	-2.57984E-04	2.26933E-03	-1.27036E-03	1.39124E+00
8	6.75000E-01	upper	2.09898E+02	1.26073E+01	-1.74132E+01	1.64085E-03	3.70492E-04	-2.52732E-03	1.32763E+00
9	5.25000E-01	upper	5.48983E+01	2.25968E+01	1.74132E+01	3.70492E-04	1.64085E-03	2.52732E-03	1.33383E+00
10	3.75000E-01	upper	2.86579E+02	7.66521E+00	8.75280E+00	2.26933E-03	-2.57984E-04	1.27036E-03	1.38276E+00
11	2.25000E-01	upper	-2.17832E+01	2.75389E+01	-8.75280E+00	-2.57984E-04	2.26933E-03	-1.27036E-03	1.39124E+00
12	7.50000E-02	upper	2.09898E+02	1.26073E+01	-1.74132E+01	1.64085E-03	3.70492E-04	-2.52732E-03	1.32763E+00
13	-7.50000E-02	upper	2.09898E+02	1.26073E+01	-1.74132E+01	1.64085E-03	3.70492E-04	-2.52732E-03	1.32763E+00
14	-2.25000E-01	upper	-2.17832E+01	2.75389E+01	-8.75280E+00	-2.57984E-04	2.26933E-03	-1.27036E-03	1.39124E+00
15	-3.75000E-01	upper	2.86579E+02	7.66521E+00	8.75280E+00	2.26933E-03	-2.57984E-04	1.27036E-03	1.38276E+00
16	-5.25000E-01	upper	5.48983E+01	2.25968E+01	1.74132E+01	3.70492E-04	1.64085E-03	2.52732E-03	1.33383E+00
17	-6.75000E-01	upper	2.09898E+02	1.26073E+01	-1.74132E+01	1.64085E-03	3.70492E-04	-2.52732E-03	1.32763E+00
18	-8.25000E-01	upper	-2.17832E+01	2.75389E+01	-8.75280E+00	-2.57984E-04	2.26933E-03	-1.27036E-03	1.39124E+00
19	-9.75000E-01	upper	2.86579E+02	7.66521E+00	8.75280E+00	2.26933E-03	-2.57984E-04	1.27036E-03	1.38276E+00
20	-1.12500E+00	upper	5.48983E+01	2.25968E+01	1.74132E+01	3.70492E-04	1.64085E-03	2.52732E-03	1.33383E+00
21	-1.27500E+00	upper	2.09898E+02	1.26073E+01	-1.74132E+01	1.64085E-03	3.70492E-04	-2.52732E-03	1.32763E+00
22	-1.42500E+00	upper	-2.17832E+01	2.75389E+01	-8.75280E+00	-2.57984E-04	2.26933E-03	-1.27036E-03	1.39124E+00
23	-1.57500E+00	upper	2.86579E+02	7.66521E+00	8.75280E+00	2.26933E-03	-2.57984E-04	1.27036E-03	1.38276E+00
24	-1.72500E+00	upper	5.48983E+01	2.25968E+01	1.74132E+01	3.70492E-04	1.64085E-03	2.52732E-03	1.33383E+00

Figure 2.23 Stresses and strains in the local reference frame, Failure index (Tsai-Hill) obtained with Elamx2 (Initial Laminate).

In figures 2.21, 2.22, 2.24, the stress and strain states in the global and local reference frames are shown, along with the failure indices calculated using different criteria for the various plies. It is observed that the global strains are constant through the thickness because only membrane loads (N) are applied, resulting in zero curvatures ($\kappa = 0$). It is also noted that using Maximum Stress or Maximum Strain criteria yields a minimum Failure Index corresponding to M.S. $\approx$ 0.5 (F.I. $\approx$ 1.5). However, under these loading conditions, the quadratic (interactive) criteria (Tsai-Hill, Tsai-Wu) are more conservative,

lamina	seq_theta	MaxStress	MaxStrain	TsaiHill	TsaiWu
1	0	1.8321	1.9813	1.3338	1.5380
2	45	1.5144	1.5300	1.3828	1.7105
3	-45	1.5033	1.4595	1.3912	1.3554
4	90	1.9813	1.9813	1.3276	1.7618
5	0	1.8321	1.9813	1.3338	1.5380
6	45	1.5144	1.5300	1.3828	1.7105
7	-45	1.5033	1.4595	1.3912	1.3554
8	90	1.9813	1.9813	1.3276	1.7618
9	0	1.8321	1.9813	1.3338	1.5380
10	45	1.5144	1.5300	1.3828	1.7105
11	-45	1.5033	1.4595	1.3912	1.3554
12	90	1.9813	1.9813	1.3276	1.7618
13	90	1.9813	1.9813	1.3276	1.7618
14	-45	1.5033	1.4595	1.3912	1.3554
15	45	1.5144	1.5300	1.3828	1.7105
16	0	1.8321	1.9813	1.3338	1.5380
17	90	1.9813	1.9813	1.3276	1.7618
18	-45	1.5033	1.4595	1.3912	1.3554
19	45	1.5144	1.5300	1.3828	1.7105
20	0	1.8321	1.9813	1.3338	1.5380
21	90	1.9813	1.9813	1.3276	1.7618
22	-45	1.5033	1.4595	1.3912	1.3554
23	45	1.5144	1.5300	1.3828	1.7105
24	0	1.8321	1.9813	1.3338	1.5380

Figure 2.24 Calculated Failure Indices using Maximum Stress, Maximum Strain, Tsai-Hill, Tsai-Wu criteria for each ply (Initial Laminate).

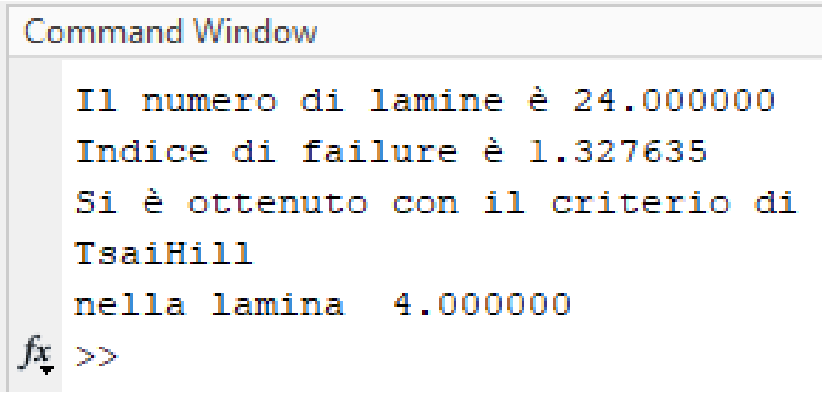

Figure 2.25 Summary Result: Minimum Margin of Safety (Initial Laminate).

yielding lower margins. Specifically, Fig.2.25 shows that the minimum Failure Index (highest risk) occurs with the Tsai-Hill criterion in the fourth ply (likely the 0° ply in the [90/45/−45/0] repeating unit) and is approximately 1.33. The corresponding Margin of

Safety is:

$$M.S. = \frac{1}{F.I.} - 1 = \frac{1}{1.33} - 1 \approx 0.75 - 1 = -0.25 \tag{2.14}$$

This margin (0.33) is slightly lower than the desired margin of 0.5.

Therefore, the laminate can be modified, for example, by adding extra ±45° plies to the outer surfaces (which might improve shear performance and damage tolerance). The results for such a modified laminate are reported below:

Stress e deformazioni nel riferimento globale

lamina	seq_theta	σx	σy	τxy	εx	εy	γxy
1	45	1.1098e+08	1.2745e+08	1.1200e+08	2.5337e-04	0.0014	0.0020
2	-45	-5.1414e+05	1.5964e+07	1.4875e+07	2.5400e-04	0.0014	0.0020
3	0	3.9288e+07	1.9628e+07	1.3489e+07	2.5464e-04	0.0015	0.0020
4	45	1.1134e+08	1.2783e+08	1.1235e+08	2.5527e-04	0.0015	0.0020
5	-45	-5.2312e+05	1.5970e+07	1.4944e+07	2.5590e-04	0.0015	0.0020
6	90	1.0260e+07	1.8562e+08	1.3533e+07	2.5653e-04	0.0015	0.0020
7	0	3.9628e+07	1.9690e+07	1.3548e+07	2.5716e-04	0.0015	0.0020
8	45	1.1182e+08	1.2832e+08	1.1281e+08	2.5780e-04	0.0015	0.0020
9	-45	-5.3510e+05	1.5978e+07	1.5037e+07	2.5843e-04	0.0015	0.0020
10	90	1.0311e+07	1.8614e+08	1.3592e+07	2.5906e-04	0.0015	0.0020
11	0	3.9968e+07	1.9753e+07	1.3607e+07	2.5969e-04	0.0015	0.0020
12	45	1.1229e+08	1.2882e+08	1.1328e+08	2.6032e-04	0.0015	0.0020
13	-45	-5.4707e+05	1.5986e+07	1.5129e+07	2.6096e-04	0.0015	0.0020
14	90	1.0363e+07	1.8665e+08	1.3651e+07	2.6159e-04	0.0015	0.0020
15	90	1.0376e+07	1.8678e+08	1.3666e+07	2.6222e-04	0.0015	0.0020
16	-45	-5.5605e+05	1.5992e+07	1.5199e+07	2.6285e-04	0.0015	0.0020
17	45	1.1289e+08	1.2944e+08	1.1386e+08	2.6348e-04	0.0015	0.0020
18	0	4.0562e+07	1.9863e+07	1.3710e+07	2.6412e-04	0.0015	0.0020
19	90	1.0427e+07	1.8730e+08	1.3725e+07	2.6475e-04	0.0015	0.0020
20	-45	-5.6802e+05	1.6000e+07	1.5291e+07	2.6538e-04	0.0015	0.0020
21	45	1.1337e+08	1.2994e+08	1.1432e+08	2.6601e-04	0.0015	0.0020
22	0	4.0902e+07	1.9925e+07	1.3769e+07	2.6664e-04	0.0015	0.0020
23	90	1.0478e+07	1.8782e+08	1.3784e+07	2.6728e-04	0.0015	0.0020
24	-45	-5.8000e+05	1.6008e+07	1.5384e+07	2.6791e-04	0.0015	0.0020
25	45	1.1384e+08	1.3044e+08	1.1479e+08	2.6854e-04	0.0015	0.0020
26	0	4.1242e+07	1.9988e+07	1.3828e+07	2.6917e-04	0.0015	0.0020
27	45	1.1408e+08	1.3069e+08	1.1502e+08	2.6980e-04	0.0015	0.0020
28	-45	-5.9197e+05	1.6016e+07	1.5477e+07	2.7044e-04	0.0015	0.0020

Figure 2.26 Calculated Stresses and Strains in the Global (x-y) Reference Frame (Modified Laminate).

Stress e deformazioni nel riferimento locale

lamina	seq_theta	σ1	σ2	τ12	ε1	ε2	γ12
1	45	2.3122e+08	7.2158e+06	8.2365e+06	0.0018	-1.2564e-04	0.0012
2	-45	-7.1498e+06	2.2599e+07	-8.2390e+06	-1.2590e-04	0.0018	-0.0012
3	0	3.9288e+07	1.9628e+07	1.3489e+07	2.5464e-04	0.0015	0.0020
4	45	2.3193e+08	7.2332e+06	8.2440e+06	0.0018	-1.2642e-04	0.0012
5	-45	-7.2208e+06	2.2667e+07	-8.2465e+06	-1.2668e-04	0.0018	-0.0012
6	90	1.8562e+08	1.0260e+07	-1.3533e+07	0.0015	2.5653e-04	-0.0020
7	0	3.9628e+07	1.9690e+07	1.3548e+07	2.5716e-04	0.0015	0.0020
8	45	2.3288e+08	7.2564e+06	8.2540e+06	0.0018	-1.2745e-04	0.0012
9	-45	-7.3154e+06	2.2758e+07	-8.2565e+06	-1.2771e-04	0.0018	-0.0012
10	90	1.8614e+08	1.0311e+07	-1.3592e+07	0.0015	2.5906e-04	-0.0020
11	0	3.9968e+07	1.9753e+07	1.3607e+07	2.5969e-04	0.0015	0.0020
12	45	2.3383e+08	7.2797e+06	8.2640e+06	0.0018	-1.2848e-04	0.0012
13	-45	-7.4100e+06	2.2849e+07	-8.2665e+06	-1.2874e-04	0.0019	-0.0012
14	90	1.8665e+08	1.0363e+07	-1.3651e+07	0.0015	2.6159e-04	-0.0020
15	90	1.8678e+08	1.0376e+07	-1.3666e+07	0.0015	2.6222e-04	-0.0020
16	-45	-7.4809e+06	2.2917e+07	-8.2740e+06	-1.2951e-04	0.0019	-0.0012
17	45	2.3502e+08	7.3087e+06	8.2765e+06	0.0019	-1.2977e-04	0.0012
18	0	4.0562e+07	1.9863e+07	1.3710e+07	2.6412e-04	0.0015	0.0020
19	90	1.8730e+08	1.0427e+07	-1.3725e+07	0.0015	2.6475e-04	-0.0020
20	-45	-7.5756e+06	2.3007e+07	-8.2840e+06	-1.3055e-04	0.0019	-0.0012
21	45	2.3597e+08	7.3320e+06	8.2865e+06	0.0019	-1.3081e-04	0.0012
22	0	4.0902e+07	1.9925e+07	1.3769e+07	2.6664e-04	0.0015	0.0020
23	90	1.8782e+08	1.0478e+07	-1.3784e+07	0.0015	2.6728e-04	-0.0020
24	-45	-7.6702e+06	2.3098e+07	-8.2940e+06	-1.3158e-04	0.0019	-0.0012
25	45	2.3693e+08	7.3552e+06	8.2965e+06	0.0019	-1.3184e-04	0.0012
26	0	4.1242e+07	1.9988e+07	1.3828e+07	2.6917e-04	0.0015	0.0020
27	45	2.3740e+08	7.3668e+06	8.3015e+06	0.0019	-1.3235e-04	0.0012
28	-45	-7.7648e+06	2.3189e+07	-8.3040e+06	-1.3261e-04	0.0019	-0.0012

Figure 2.27 Calculated Stresses and Strains in the Local (1-2) Reference Frame for each ply (Modified Laminate).

Local layer results :

No.	zmi		s11	s22	s12	e11	e22	e12	RF
1	2.02500K+00	upper	2.31100K+02	7.21281K+00	8.23522K+00	1.82687K-03	-1.25518K-04	1.19524K-03	1.66200K+00
		lower	2.31337K+02	7.21863K+00	8.23772K+00	1.82875K-03	-1.25776K-04	1.19561K-03	1.66050K+00
2	1.87500K+00	upper	-7.13846K+00	2.25882K+01	-8.23772K+00	-1.25776K-04	1.82875K-03	-1.19561K-03	1.67450K+00
		lower	-7.16211K+00	2.26108K+01	-8.24022K+00	-1.26034K-04	1.83064K-03	-1.19597K-03	1.67300K+00
3	1.72500K+00	upper	3.92454K+01	1.96199K+01	1.34815K+01	2.54319K-04	1.45029K-03	1.95667K-03	1.61928K+00
		lower	3.93304K+01	1.96356K+01	1.34962K+01	2.54951K-04	1.45128K-03	1.95882K-03	1.61776K+00
4	1.57500K+00	upper	2.31813K+02	7.23025K+00	8.24272K+00	1.83252K-03	-1.26292K-04	1.19633K-03	1.65753K+00
		lower	2.32051K+02	7.23606K+00	8.24522K+00	1.83441K-03	-1.26550K-04	1.19669K-03	1.65604K+00
5	1.42500K+00	upper	-7.20942K+00	2.26562K+01	-8.24522K+00	-1.26550K-04	1.83441K-03	-1.19669K-03	1.67000K+00
		lower	-7.23307K+00	2.26788K+01	-8.24772K+00	-1.26808K-04	1.83629K-03	-1.19706K-03	1.66850K+00
6	1.27500K+00	upper	1.85555K+02	1.02538K+01	-1.35258K+01	1.45327K-03	2.56215K-04	-1.96310K-03	1.60594K+00
		lower	1.85685K+02	1.02666K+01	-1.35405K+01	1.45427K-03	2.56847K-04	-1.96525K-03	1.60444K+00
7	1.12500K+00	upper	3.95853K+01	1.96826K+01	1.35405K+01	2.56847K-04	1.45427K-03	1.96525K-03	1.61322K+00
		lower	3.96702K+01	1.96982K+01	1.35553K+01	2.57479K-04	1.45526K-03	1.96739K-03	1.61171K+00
8	9.75000K-01	upper	2.32764K+02	7.25349K+00	8.25272K+00	1.84006K-03	-1.27324K-04	1.19778K-03	1.65160K+00
		lower	2.33002K+02	7.25930K+00	8.25522K+00	1.84195K-03	-1.27583K-04	1.19814K-03	1.65013K+00
9	8.25000K-01	upper	-7.30402K+00	2.27468K+01	-8.25522K+00	-1.27583K-04	1.84195K-03	-1.19814K-03	1.66403K+00
		lower	-7.32768K+00	2.27695K+01	-8.25772K+00	-1.27841K-04	1.84383K-03	-1.19851K-03	1.66254K+00
10	6.75000K-01	upper	1.86072K+02	1.03050K+01	-1.35848K+01	1.45725K-03	2.58743K-04	-1.97168K-03	1.59996K+00
		lower	1.86201K+02	1.03179K+01	-1.35996K+01	1.45825K-03	2.59376K-04	-1.97382K-03	1.59847K+00
11	5.25000K-01	upper	3.99251K+01	1.97452K+01	1.35996K+01	2.59376K-04	1.45825K-03	1.97382K-03	1.60720K+00
		lower	4.00101K+01	1.97609K+01	1.36144K+01	2.60008K-04	1.45924K-03	1.97596K-03	1.60570K+00
12	3.75000K-01	upper	2.33716K+02	7.27674K+00	8.26271K+00	1.84760K-03	-1.28357K-04	1.19923K-03	1.64572K+00
		lower	2.33954K+02	7.28255K+00	8.26521K+00	1.84949K-03	-1.28615K-04	1.19960K-03	1.64425K+00
13	2.25000K-01	upper	-7.39863K+00	2.28375K+01	-8.26521K+00	-1.28615K-04	1.84949K-03	-1.19960K-03	1.65809K+00
		lower	-7.42228K+00	2.28601K+01	-8.26771K+00	-1.28873K-04	1.85138K-03	-1.19996K-03	1.65662K+00
14	7.50000K-02	upper	1.86589K+02	1.03563K+01	-1.36439K+01	1.46123K-03	2.61272K-04	-1.98025K-03	1.59403K+00
		lower	1.86718K+02	1.03691K+01	-1.36587K+01	1.46223K-03	2.61904K-04	-1.98239K-03	1.59255K+00
15	-7.50000K-02	upper	1.86718K+02	1.03691K+01	-1.36587K+01	1.46223K-03	2.61904K-04	-1.98239K-03	1.59255K+00
		lower	1.86848K+02	1.03819K+01	-1.36734K+01	1.46322K-03	2.62536K-04	-1.98453K-03	1.59108K+00
16	-2.25000K-01	upper	-7.46959K+00	2.29055K+01	-8.27271K+00	-1.29389K-04	1.85515K-03	-1.20068K-03	1.65367K+00
		lower	-7.49324K+00	2.29281K+01	-8.27521K+00	-1.29647K-04	1.85703K-03	-1.20105K-03	1.65220K+00
17	-3.75000K-01	upper	2.34905K+02	7.30580K+00	8.27521K+00	1.85703K-03	-1.29647K-04	1.20105K-03	1.63842K+00
		lower	2.35143K+02	7.31161K+00	8.27771K+00	1.85892K-03	-1.29906K-04	1.20141K-03	1.63697K+00
18	-5.25000K-01	upper	4.05199K+01	1.98549K+01	1.37030K+01	2.63800K-04	1.46521K-03	1.98882K-03	1.59677K+00
		lower	4.06048K+01	1.98705K+01	1.37177K+01	2.64432K-04	1.46620K-03	1.99096K-03	1.59529K+00
19	-6.75000K-01	upper	1.87235K+02	1.04203K+01	-1.37177K+01	1.46620K-03	2.64432K-04	-1.99096K-03	1.58668K+00
		lower	1.87364K+02	1.04332K+01	-1.37325K+01	1.46720K-03	2.65064K-04	-1.99311K-03	1.58521K+00
20	-8.25000K-01	upper	-7.56419K+00	2.29961K+01	-8.28271K+00	-1.30422K-04	1.86269K-03	-1.20213K-03	1.64781K+00
		lower	-7.58784K+00	2.30188K+01	-8.28521K+00	-1.30680K-04	1.86457K-03	-1.20250K-03	1.64635K+00
21	-9.75000K-01	upper	2.35856K+02	7.32904K+00	8.28521K+00	1.86457K-03	-1.30680K-04	1.20250K-03	1.63262K+00
		lower	2.36094K+02	7.33485K+00	8.28771K+00	1.86646K-03	-1.30938K-04	1.20286K-03	1.63118K+00
22	-1.12500K+00	upper	4.08597K+01	1.99175K+01	1.37620K+01	2.66328K-04	1.46919K-03	1.99739K-03	1.59087K+00
		lower	4.09447K+01	1.99332K+01	1.37768K+01	2.66960K-04	1.47018K-03	1.99954K-03	1.58940K+00
23	-1.27500K+00	upper	1.87752K+02	1.04716K+01	-1.37768K+01	1.47018K-03	2.66960K-04	-1.99954K-03	1.58084K+00
		lower	1.87881K+02	1.04844K+01	-1.37916K+01	1.47118K-03	2.67592K-04	-2.00168K-03	1.57939K+00
24	-1.42500K+00	upper	-7.65880K+00	2.30868K+01	-8.29271K+00	-1.31454K-04	1.87023K-03	-1.20359K-03	1.64199K+00
		lower	-7.68245K+00	2.31094K+01	-8.29521K+00	-1.31712K-04	1.87211K-03	-1.20395K-03	1.64054K+00
25	-1.57500K+00	upper	2.36808K+02	7.35229K+00	8.29521K+00	1.87211K-03	-1.31712K-04	1.20395K-03	1.62687K+00
		lower	2.37045K+02	7.35810K+00	8.29771K+00	1.87400K-03	-1.31970K-04	1.20431K-03	1.62543K+00
26	-1.72500K+00	upper	4.11995K+01	1.99802K+01	1.38211K+01	2.68857K-04	1.47317K-03	2.00597K-03	1.58501K+00
		lower	4.12845K+01	1.99958K+01	1.38359K+01	2.69489K-04	1.47416K-03	2.00811K-03	1.58356K+00
27	-1.87500K+00	upper	2.37283K+02	7.36391K+00	8.30021K+00	1.87588K-03	-1.32229K-04	1.20467K-03	1.62400K+00
		lower	2.37521K+02	7.36972K+00	8.30271K+00	1.87777K-03	-1.32487K-04	1.20504K-03	1.62258K+00
28	-2.02500K+00	upper	-7.75341K+00	2.31774K+01	-8.30271K+00	-1.32487K-04	1.87777K-03	-1.20504K-03	1.63621K+00
		lower	-7.77706K+00	2.32001K+01	-8.30520K+00	-1.32745K-04	1.87965K-03	-1.20540K-03	1.63477K+00

Figure 2.28 Stresses and strains in the local reference frame, Failure index (Tsai-Wu shown) obtained with Elamx2 (Modified Laminate).

Indici di Failure, con diversi criteri

lamina	seq_theta	MaxStress	MaxStrain	TsaiHill	TsaiWu
1	45	1.8770	1.8995	1.6613	2.1100
2	-45	1.8319	1.8101	1.6738	1.6737
3	0	2.1093	2.2829	1.6185	1.8373
4	45	1.8712	1.8937	1.6568	2.1042
5	-45	1.8264	1.8046	1.6693	1.6690
6	90	2.3381	2.3883	1.6052	2.1449
7	0	2.1025	2.2767	1.6125	1.8313
8	45	1.8636	1.8859	1.6509	2.0965
9	-45	1.8191	1.7972	1.6633	1.6626
10	90	2.3316	2.3818	1.5992	2.1372
11	0	2.0959	2.2704	1.6065	1.8253
12	45	1.8560	1.8782	1.6450	2.0889
13	-45	1.8119	1.7899	1.6574	1.6563
14	90	2.3252	2.3753	1.5933	2.1296
15	90	2.3236	2.3737	1.5918	2.1277
16	-45	1.8065	1.7844	1.6529	1.6516
17	45	1.8466	1.8687	1.6377	2.0795
18	0	2.0843	2.2597	1.5960	1.8150
19	90	2.3171	2.3672	1.5859	2.1202
20	-45	1.7994	1.7772	1.6471	1.6454
21	45	1.8392	1.8612	1.6319	2.0720
22	0	2.0778	2.2535	1.5901	1.8091
23	90	2.3108	2.3608	1.5801	2.1127
24	-45	1.7924	1.7700	1.6413	1.6393
25	45	1.8318	1.8537	1.6262	2.0646
26	0	2.0712	2.2475	1.5843	1.8032
27	45	1.8281	1.8499	1.6233	2.0609
28	-45	1.7853	1.7629	1.6355	1.6332

Figure 2.29 Calculated Failure Indices using various criteria for each ply (Modified Laminate).

```
Il numero di lamine è 28.000000
Lo spessore è 0.004200 m
 Indice di failure è 1.580115
Si è ottenuto con il criterio di
TsaiHill
nella lamina  23.000000
fx >>
```

Figure 2.30 Summary Result: Minimum Margin of Safety (Modified Laminate).

Chapter 3

Kirchhoff Plate Theory and Buckling

3.1 Introduction to Kirchhoff Plate Theory

The plate is one of the fundamental components of aeronautical structures because it allows realizing the necessary shapes for the aircraft to ensure desired aerodynamic performance while simultaneously absorbing the loads acting upon it. One of the most widespread theories for describing the behavior of plates is the Kirchhoff plate theory. This represents a simplification of general plate theory but, despite this, is sufficiently reliable in many aeronautical applications. The assumptions underlying this theory are similar to those discussed for Classical Lamination Theory, in particular, it is assumed that: the thickness is small compared to the other two dimensions; displacements are small compared to the plate thickness; lines initially straight and normal to the neutral surface remain straight and normal to the surface even after deformation (Kirchhoff Hypothesis).

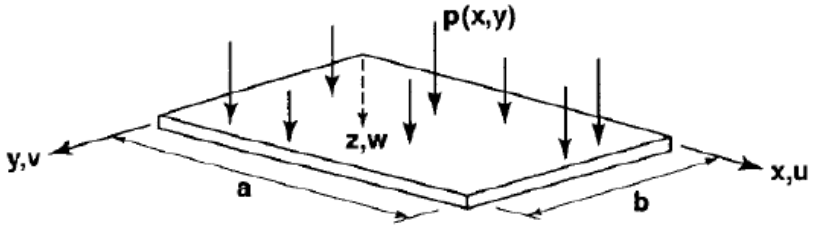

Figure 3.1 Thin plate subjected to transverse loads.

3.2 Kirchhoff Plate Subjected to Pressure Load

3.2.1 Isotropic Materials Case

In the case of isotropic materials, the problem of a Kirchhoff plate subjected to a transverse pressure load can be described analytically by the following expression:

$$\frac{\partial^4 w}{\partial x^4} + 2\frac{\partial^4 w}{\partial x^2 \partial y^2} + \frac{\partial^4 w}{\partial y^4} = \frac{q(x,y)}{D} \tag{3.1}$$

Where w represents the displacement in the direction normal to the plate, $q(x,y)$ is an arbitrary pressure load distribution as shown in Fig.3.1. D is the flexural rigidity (or bending stiffness) of the plate and takes this expression:

$$D = \frac{Eh^3}{12(1-\nu^2)} \tag{3.2}$$

ν is the Poisson's ratio of the isotropic material, E is the Young's modulus (unique for isotropic material), and h is the thickness of the plate. To solve this fourth-order partial differential equation, boundary conditions must be assigned, i.e., support conditions. In the case of a "simply supported" plate, meaning supported on all four sides, the boundary conditions are written as:

$$\begin{aligned} &w(x=0)=0, \quad w(x=a)=0 \\ &\left.\frac{\partial^2 w}{\partial x^2}\right|_{x=0} = 0, \quad \left.\frac{\partial^2 w}{\partial x^2}\right|_{x=a} = 0 \\ &w(y=0)=0, \quad w(y=b)=0 \\ &\left.\frac{\partial^2 w}{\partial y^2}\right|_{y=0} = 0, \quad \left.\frac{\partial^2 w}{\partial y^2}\right|_{y=b} = 0 \end{aligned} \tag{3.3}$$

Where a and b indicate the dimensions of the plate. The solution for this particular case can be found using Navier's double sine series expansion:

$$w(x,y) = \frac{1}{\pi^4 D}\sum_{m=1}^{\infty}\sum_{n=1}^{\infty}\frac{a_{mn}}{\left[(\frac{m}{a})^2+(\frac{n}{b})^2\right]^2}\sin\frac{m\pi x}{a}\sin\frac{n\pi y}{b} \tag{3.4}$$

where the coefficients a_{mn} are determined from the load distribution $q(x,y)$:

$$a_{mn} = \frac{4}{ab}\int_0^a\int_0^b q(x,y)\sin\frac{m\pi x}{a}\sin\frac{n\pi y}{b}\mathrm{d}x\mathrm{d}y \tag{3.5}$$

In the case of a uniformly distributed load, $q(x,y) = q_0$, the solution can be written in the form:

$$w(x,y) = \frac{16q_0}{\pi^6 D}\sum_{m=1,3,5}^{\infty}\sum_{n=1,3,5}^{\infty}\frac{\sin(m\pi x/a)\sin(n\pi y/b)}{mn[(m/a)^2+(n/b)^2]^2} \tag{3.6}$$

3.2.2 Specially Orthotropic Composite Laminate Case

In the case of composite materials, obtaining a simple analytical formulation for the problem is generally not possible. The main reason is that the material is anisotropic (or orthotropic), and thus there isn't a single flexural rigidity constant D. This means that the equations for vertical equilibrium and rotational equilibrium around the x and y axes become coupled. Generally, it will be necessary to resort to numerical solutions using software like, for example, Femap. Specially orthotropic composite laminates are an exception; for these, the only non-zero coefficients of the [D] submatrix of the ABD matrix are D_{11}, D_{22}, D_{12} (= D_{21}), and D_{66} (assuming a symmetric laminate, otherwise [B] might exist but is often zero for specially orthotropic layups relevant here). For these, the problem can be described by the following equation:

$$D_{11}\frac{\partial^4 w}{\partial x^4} + 2(D_{12} + 2D_{66})\frac{\partial^4 w}{\partial x^2 \partial y^2} + D_{22}\frac{\partial^4 w}{\partial y^4} = q(x,y) \tag{3.7}$$

where D_{ij} are the components of the bending stiffness matrix [D].

In the particular case where the load is uniform ($q(x,y) = q_0$) and the plate is simply supported, the solution using Navier's method is:

$$w(x,y) = \frac{16q_0}{\pi^6}\sum_{m=1,3,5}^{\infty}\sum_{n=1,3,5}^{\infty}\frac{\sin(m\pi x/a)\sin(n\pi y/b)}{mn\left[D_{11}(\frac{m}{a})^4 + 2(D_{12}+2D_{66})(\frac{m}{a})^2(\frac{n}{b})^2 + D_{22}(\frac{n}{b})^4\right]} \tag{3.8}$$

An example of a specially orthotropic laminate is a symmetric cross-ply laminate with sequence $[0°/90°]_{ns}$.

3.3 Transverse Load: Comparison between Isotropic Material and Composite Material

Below, a MATLAB code is presented that allows evaluating the analytical solution for the elastic deformation of a laminate made of Graphite/Epoxy BMS 8-212 Type II Class 1 composite material, previously seen in earlier chapters, with properties shown in Table 3.1.

Property	Value
E_1	125 GPa
E_2	12.5 GPa
G_{12}	6.89 GPa
ν_{12}	0.38
ν_{21}	0.038
ρ (Density)	1400 kg/m^3

Table 3.1 Graphite/Epoxy Properties

We study the laminate under the assumptions of being simply supported, subjected

to a uniform load q_0, and with assigned dimensions a and b as in Table 3.2. A stacking sequence of $[0°/90°]_{4s}$ is considered. This is a symmetric cross-ply laminate, which is specially orthotropic, so relation (3.8) is used. The summation is evaluated considering only the first few terms because it converges rapidly.

a (Length)	400 mm
b (Width)	400 mm
q_0 (Uniform pressure)	-100 Pa

Table 3.2 Dimensions and Load

The code also allows studying the elastic deformation of an aluminum plate with properties shown in Table 3.3.

Property	Value
E (Young's Modulus)	70 GPa
G (Shear Modulus)	27 GPa
ν (Poisson's Ratio)	0.33
ρ (Density)	2700 kg/m^3

Table 3.3 Aluminum Properties

The aluminum plate is assumed to have the same dimensions as the composite plate, the same boundary conditions, and the same load. The thickness of the aluminum plate required to achieve the same maximum displacement as the composite plate is evaluated, and then the weights of the two plates are compared.

Listing 3.1 MATLAB code for comparing composite and aluminum plate deflection.

```
clc; clear all; close all;
%%%%%%%%%%%%%%%%%%%%%%%%%%%%%%%%%%%%%%%%%%%%%%%%%%%%%%%%%%%%%%%%%%%%%%%%%%%%%%%
% DEFINIZIONE DEL PROBLEMA %
%%%%%%%%%%%%%%%%%%%%%%%%%%%%%%%%%%%%%%%%%%%%%%%%%%%%%%%%%%%%%%%%%%%%%%%%%%%%%%%
% Dati geometria
a = 400; % [mm]
b = 400; % [mm]
t_ply = 0.15*16; % [mm]
%Dati materiale
Dx = 9.27*10^4; % Rigidezza flessionale [N*mm]
Dy = 6.805*10^4; % Rigidezza flessionale [N*mm]
Dxy = 5.55*10^3; % Rigidezza flessionale [N*mm]
Ds = 7.94*10^3; % Rigidezza flessionale [N*mm]
H = Dxy+2*Ds;
%Carico costante
q = -0.0001; % carico di pressione [MPa]
n_passi = 700;
X = linspace (0,a,n_passi); %N.B il numero di passi deve essere lo stesso
Y = linspace (0,b,n_passi);
% Inizializzazione
```

```
w_tot = zeros(n_passi);
w1 = zeros(n_passi);
n_interazioni = 13;
n_m = ceil(n_interazioni/2);
vettore_w = zeros(1,n_m);
h = 1;
M = linspace(1,n_m,n_m);

% Doppia serie
for n=1:2:n_interazioni
for m = 1:2:n_interazioni
w = (16*q)/(pi^6)*((1/(m*n))*sin(m.*pi.*X./a).*sin(n.*pi.*Y./b)')/...
(Dx*(m/a)^4+2*H*(m/a)^2*(n/b)^2+Dy*(n/b)^4);
w1 = w;
w_tot = w_tot+w;
if (m == n)
minimo = min(min(w_tot));
vettore_w(h)=minimo;
h = h+1;
disp (['w', num2str(m), '(a/2,b/2) = ', num2str(minimo)]);
end
end
end

%%%%%%%%%%%%%%%%%%%%%%%%%%%%%%%%%%%%%%%%%%%%%%%%%%%%%%%%%%%%%%%%%%%%%%%%%%%%%%%
% PLOT % %%%%%%%%%%%%%%%%%%%%%%%%%%%%%%%%%%%%%%%%%%%%%%%%%%%%%%%%%%%%%%%%%%%%%%%
%%%%%%%%%
[X,Y] = meshgrid (X,Y);
figure
mesh(X,Y,w_tot);
xlabel([ '$' 'x\ (mm) ' '$'] ,'interpreter','latex');
ylabel([ '$' 'y\ (mm)' '$'] ,'interpreter','latex');
zlabel([ '$' 'w\ (mm)' '$'] ,'interpreter','latex');
figure
plot (M,vettore_w,'o-b', 'Linewidth' ,1.5);
grid on;
hold on
xlabel([ '$' 'm\ ' '$'] ,'interpreter','latex');
ylabel([ '$' 'w(x,y)\ (mm)' '$'] ,'interpreter','latex');


%%
%
    %%%%%%%%%%%%%%%%%%%%%%%%%%%%%%%%%%%%%%%%%%%%%%%%%%%%%%%%%%%%%%%%%%%%%%%%%%%%%%%


%%%%%%%%%%%%%%%%%%%%%%%%%%    PIASTRA ALLUMINIO
    %%%%%%%%%%%%%%%%%%%%

%
    %%%%%%%%%%%%%%%%%%%%%%%%%%%%%%%%%%%%%%%%%%%%%%%%%%%%%%%%%%%%%%%%%%%%%%%%%%%%%%%


%%
 %% Dati geometria
a = 400; % [mm]
b = 400; % [mm]
```

```
%t_tot = 2.4; % [mm]

%% Dati materiale
E = 70000; %% [MPa]
ni = 0.33; % Modulo di Poisson
coef_analitico = 0.04343;
t_tot = (abs(coef_analitico*q*(a^4)/(E*minimo)))^(1/3); % [mm]
% t_tot = 2.4;
D = (E*t_tot^3)/(12*(1-ni^2)); % Rigidezza flesisonale [N*mm]


%% Discretizzazione
n_passi = 700;
X = linspace (0,a,n_passi); %il numero di passi deve essere lo stesso
Y = linspace (0,b,n_passi);

%% Inizializzazione
w_tot = zeros(n_passi);
w1 = zeros(n_passi);
n_interazioni = 13;
n_m = ceil(n_interazioni/2);
vettore_w = zeros(1,n_m);


h = 1;
M = linspace(1,n_m,n_m);

%%Doppia serie
for n=1:2:n_interazioni
for m = 1:2:n_interazioni
w = (16*q)/(D*pi^6)*((1/(m*n))*sin(m.*pi.*X./a).*sin(n.*pi.*Y./b)')/...
 (((m/a)^2+(n/b)^2)^2);
w1 = w;
w_tot = w_tot+w;
if (m == n)
minimo = min(min(w_tot));
vettore_w(h)=minimo;
h = h+1;
disp (['w', num2str(m), '(a/2,b/2) = ', num2str(minimo)]);
end
end
end

%%%%%%%%%%%%%%%%%%%%%%%%%%%%%%%%%%%%%%%%%%%%%%%%%%%%%%%%%%%%%%%%%%%%%%%%%%
% PLOT % %%%%%%%%%%%%%%%%%%%%%%%%%%%%%%%%%%%%%%%%%%%%%%%%%%%%%%%%%%%%%%%%
%%%%%%%%%
[X,Y] = meshgrid (X,Y);
figure
mesh(X,Y,w_tot);
xlabel([ '$' 'x\ (mm) ' '$'] ,'interpreter','latex');
ylabel([ '$' 'y\ (mm)' '$'] ,'interpreter','latex');
zlabel([ '$' 'w\ (mm)' '$'] ,'interpreter','latex');
figure
plot (M,vettore_w,'o-b', 'Linewidth' ,1.5);
grid on;
hold on
```

```
xlabel([ '$' 'm\ ' '$'] ,'interpreter','latex');
ylabel([ '$' 'w(x,y)\ (mm)' '$'] ,'interpreter','latex');

%
    %%%%%%%%%%%%%%%%%%%%%%%%%%%%%%%%%%%%%%%%%%%%%%%%%%%%%%%%%%%%%%%%%%%%%%%%%%
%% Confronto tra i pesi   %%%%%%%%%%%%%%%%%%%%%%%%%%%%%%%%%%%%%%
%
    %%%%%%%%%%%%%%%%%%%%%%%%%%%%%%%%%%%%%%%%%%%%%%%%%%%%%%%%%%%%%%%%%%%%%%%%%%
Vol_comp = a * b * t_ply * 10^-9; % [m^3]
rho_comp = 1400; % [kg/m^3]
W_comp = Vol_comp * rho_comp;

Vol_al = a * b * t_tot * 10^-9; % [m^3]
rho_al = 2800; % [kg/m^3]
W_al = Vol_al * rho_al;

rapp = W_comp/W_al;
disp (['Peso pistra in alluminio:', num2str(W_al),'kg']);
disp (['Peso pistra in composito:', num2str(W_comp),'kg']);
disp (['Rapporto pesi :', num2str(rapp)]);
```

The results are shown in Figures 3.2, 3.3, 3.4, and 3.5. The result obtained with the MATLAB code is also verified against the result obtained with the Elamx2 software (Fig. 3.4). In particular, from Fig.3.2, we can observe that:

- The maximum displacement, occurring at the center of the plate, is small compared to the thickness of the plates themselves (less than one-tenth). Therefore, Kirchhoff plate theory can be applied without introducing large errors.

- The aluminum plate (with matched displacement) is thicker than the composite plate, implying the composite is stiffer per unit thickness for this layup and loading. (Note: The original text states aluminum is "more resistant" requiring "less thickness". This seems contradictory to the final weight comparison and likely means aluminum needs *more* thickness for the same displacement, hence it's less stiff per unit thickness but denser). Let's re-evaluate based on the weight conclusion: If the composite is lighter for the same displacement, it must either be thinner or significantly less dense. Given the stiffness values, the composite ($[0/90]_{4s}$) might be stiffer overall than aluminum despite lower E_2. Let's assume the text meant the aluminum plate needs to be *thicker* to match the composite displacement. Revised interpretation: The composite plate requires a total thickness of $16 \times t_{ply} = 16 \times 0.15 = 2.4$ mm. The aluminum plate requires a thickness of 2.96 mm to match the displacement.

- Although the composite plate might be less stiff than aluminum if thicknesses were equal (depending on the specific comparison), for the same maximum displacement (meaning the aluminum plate is thicker), the composite plate is significantly lighter: its weight is about 60 percent of the equivalent aluminum plate. This highlights the weight-saving potential of composites.

```
Massimo spostamento in entrambi casi: -0.20565mm
Spessore piastra in compodito: 2.4mm
Spessore piastra in alluminio: 1.9768mm
Peso piastra in alluminio: 0.88561mm
Peso pistra in composito: 0.5376kg
Rapporto pesi: 0.60704
fx >>
```

Figure 3.2 Results in terms of displacement, thicknesses, and weight comparison.

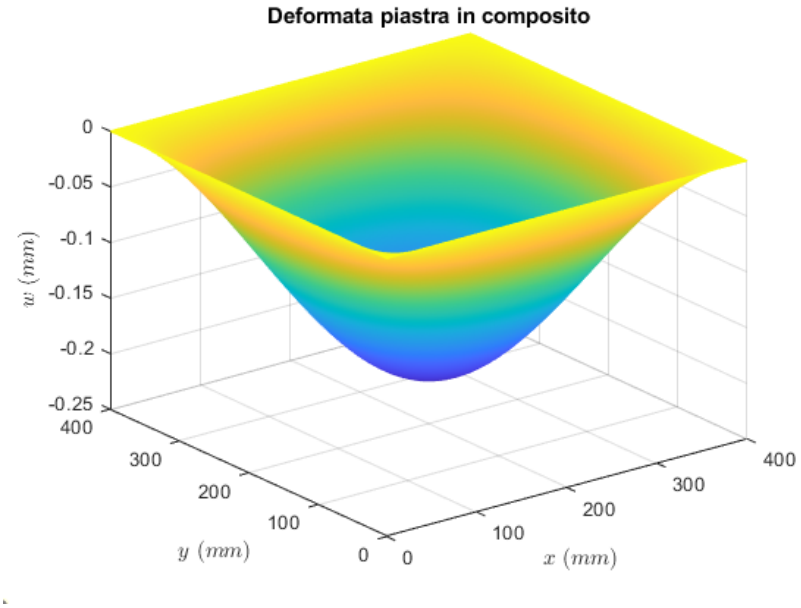

Figure 3.3 Deformed shape of the composite plate (MATLAB).

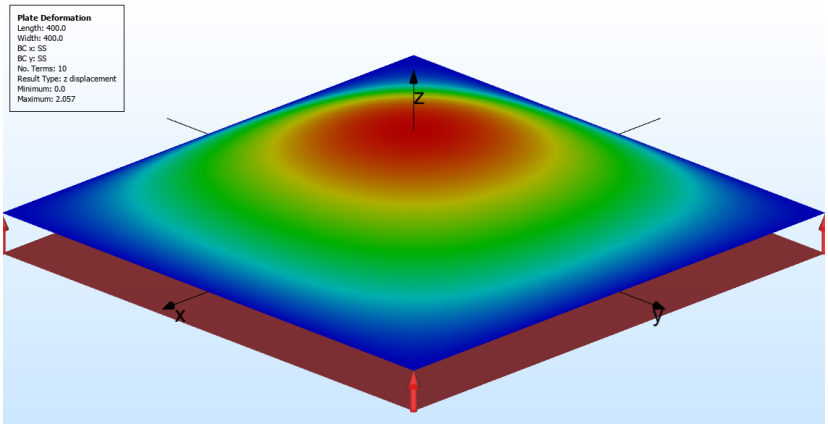

Figure 3.4 Deformed shape of the composite plate obtained with Elamx2.

3.4 Applicability Limits of Kirchhoff Theory and Comparison of Different Lamination Sequences

In the previous section, the analytical solution of the Kirchhoff plate model was reconstructed. Clearly, this theory has applicability limits. In particular, it produces unreliable results for thick plates where transverse shear deformations and normal stresses (σ_z) are not negligible, and it is not effective for high loads that lead to displacements greater than about one-tenth of the plate thickness (violating the small displacement assumption,

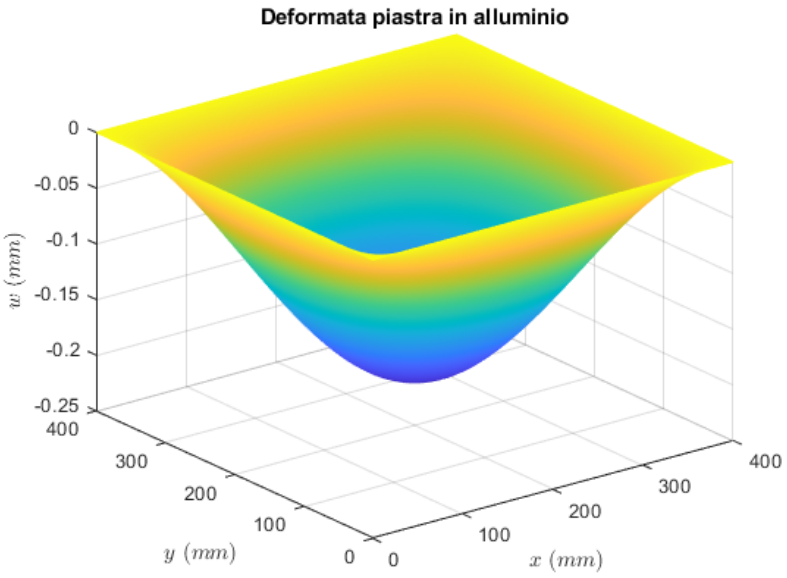

Figure 3.5 Deformed shape of the aluminum plate (MATLAB).

potentially entering geometric non-linearity). We study again the problem of the simply-supported plate subjected to uniform pressure load. We consider the same materials and geometries as in the previous section (Tables 3.1, 3.2, 3.3), but this time using the Femap software. With finite element analysis (FEA), using a sufficiently refined mesh, more accurate results are obtained that are not based on simplifying assumptions about the negligibility of shear.

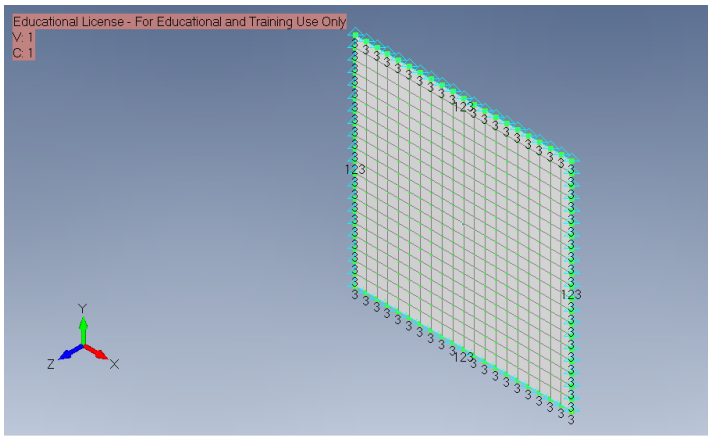

Figure 3.6 FEA Mesh and boundary conditions in Femap.

From the results shown in Fig. 3.8 and Fig. 3.9, it is observed that the maximum displacements for the composite and aluminum plates are $w_c \approx 0.2059$ mm and $w_{al} \approx 0.2061$ mm, respectively. Comparing with the analytical results (e.g., $w_{c,analytical} \approx 0.2054$ mm from Fig. 3.2), the relative errors are approximately $e_c \approx 0.24\%$ and $e_{al} \approx 0.15\%$. The errors made using the analytical model are engineeringly negligible because the thicknesses used are indeed small compared to the in-plane dimensions. Below, Table 3.10 and Fig. 3.11 show how the error of the analytical solution compared to the numerical one increases with thickness for the composite plate. It is observed that for a thickness greater than 10

We also observed in previous sections that the simple analytical solution can only

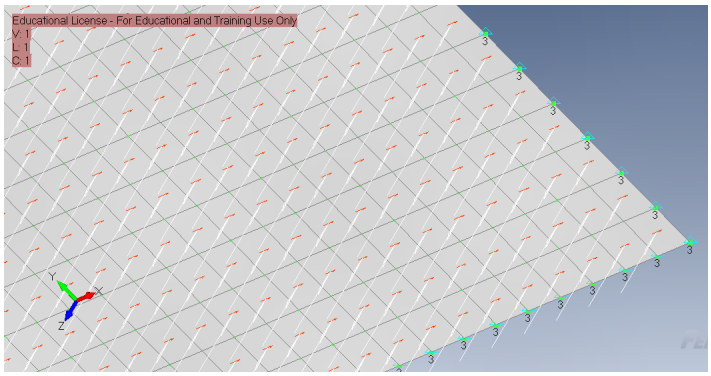

Figure 3.7 Material reference direction (red) and distributed pressure load (white) in Femap.

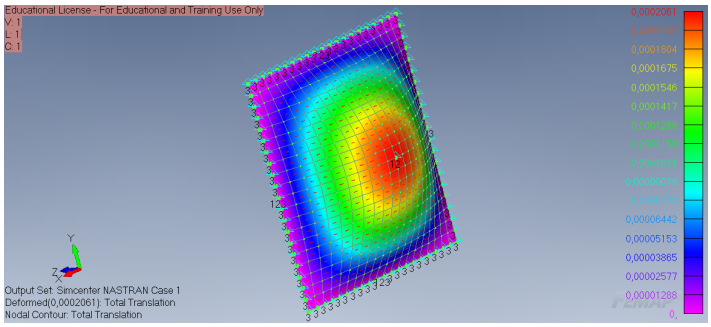

Figure 3.8 Deformation of the composite laminate (Femap).

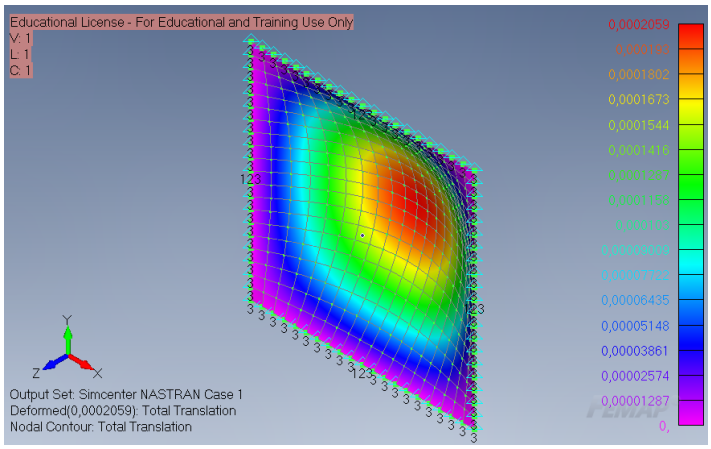

Figure 3.9 Deformed shape of the aluminum plate (Femap).

Effetto dello spessore

spessore(mm)	spessore(perc)	wFEM(mm)	wAN(mm)	Err(perc)
2.4000	0.6000	-0.2061	-0.2057	0.2183
12	3	-0.0017	-0.0016	1.8198
24	6	-2.1823e-04	-2.0565e-04	5.7646
36	9	-6.8153e-05	-6.0944e-05	10.5777
48	12	-3.1036e-05	-2.5711e-05	17.1575

Figure 3.10 Effect of thickness on displacement and error (Analytical vs. FEM).

be found for specially orthotropic laminates like symmetric cross-plies. In the case of laminates that are not specially orthotropic, Eq. (3.8) is not valid. However, it is sometimes used anyway, producing results with varying degrees of error depending on the laminate properties (specifically, the magnitude of D_{16} and D_{26}). Below, the solutions in terms

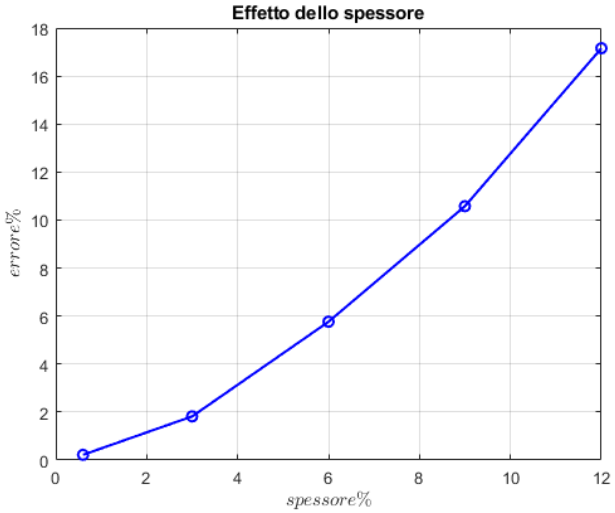

Figure 3.11 Percentage error increases with thickness.

of maximum displacement for different lamination sequences are reported, obtained with the analytical solution (using the presented MATLAB code, likely applying Eq. (3.8) even when not strictly valid) and the numerical solution (obtained with Femap), and the relative error is observed. The results are shown in Figure 3.12. In particular, it is observed that:

- Due to the symmetry of the problem in terms of load and boundary conditions for a square plate, the maximum displacement is the same for a UD laminate with all plies at 0° or all plies at 90°.
- The first 3 sequences ($[0]_{16}$, $[90]_{16}$, $[0/90]_{4s}$) are specially orthotropic laminates for which the analytical solution is exact within the Kirchhoff assumptions. Indeed, a percentage error relative to the numerical solution below 1
- The fourth ($[0/\pm45/90]_{2s}$) and fifth ($[\pm45]_{4s}$) sequences represent symmetric laminates that are generally anisotropic in bending (D_{16}, D_{26} are non-zero). For these laminates, the error using Eq. (3.8) is small but non-zero because the bending-twisting coupling terms D_{16} and D_{26} are small but not null. (Note: The error for $[\pm45]_{4s}$ is shown as 0
- The laminate

$$[\pm45^\circ/\pm45^\circ/\pm45^\circ/\pm45^\circ/0^\circ/90^\circ/0^\circ/90^\circ/0^\circ/90^\circ/0^\circ/90^\circ]$$

  is not symmetric and does not exhibit special orthotropy. For this reason, the analytical solution (Eq. (3.8)) produces a result with an error of almost 10
- It is observed that the use of plies oriented at ±45° generally increases torsional stiffness (D_{66}) and can influence bending stiffness. Comparing sequences, the quasi-isotropic laminate $[0/\pm45/90]_{2s}$ exhibits the smallest maximum displacement (highest bending stiffness) among the balanced/symmetric options shown. (Note: The original text mentions this laminate as having the best behavior).

Sequenza	wFEM(mm)	wAN(mm)	Err(perc)
[0]16	-0.2015	-0.20087	0.31266
[90]16	-0.2015	-0.20087	0.31266
[0/90]8s	-0.2061	-0.20565	0.21834
[0/+-45/90/0/90/0/90]s	-0.1656	-0.1639	1.0266
[0/+-45/90]2s	-0.16198	-0.15579	3.8215
[0/+-45/90/0/+-45/90/0/90/0/90/0/90/0/90]	-0.1889	-0.1775	6.0349
[+-45/+-45/+-45/+-45/0/90/0/90/0/90/0/90]	-0.1754	-0.15844	9.6693

Figure 3.12 Percentage error increases when considering laminates that do not exhibit special orthotropy (using Eq. 3.8).

3.5 Buckling

Buckling instability of thin plates is a structural phenomenon that occurs when a plate subjected to a compressive force loses its stable deformed shape and suddenly deforms, adopting a wavy or bent configuration. This behavior manifests when the applied force exceeds a critical threshold, causing elastic (or plastic) deformation that can compromise the functionality and safety of the structure. In general, a structure is said to be in equilibrium when the system of loads applied to it is balanced by the internal reaction system that develops. The equilibrium achieved will be stable if, in the presence of a disturbance to the equilibrium condition (which can be expressed either in terms of displacement or loads), the system responds by eliminating the disturbance and returning to the initial equilibrium condition. The system is in stable equilibrium when it is in a state of absolute minimum elastic potential energy. The phenomenon of compressive instability in thin plates occurs when the compressive load reaches a value such that the structure enters a state of neutral (or indifferent) equilibrium: in this condition, ideally, infinite elastic equilibrium shapes exist for the system, and it therefore does not tend to dampen perturbations. In practice, this means the plate deforms out of its plane even if no transverse loads or bending moments are present. The critical load and the buckling mode shape are influenced by various factors, including the plate geometry, support conditions, and material properties. In this section, the compressive buckling instability of plates is analyzed for both an isotropic material plate (aluminum is considered) and a composite material plate, considering different lamination sequences. Analytical results are compared, where possible, with those obtained from FEM analysis, and the critical buckling loads are compared.

3.5.1 Buckling: Comparison between Isotropic Material and Composite Material

The buckling problem can be approached analytically using Kirchhoff plate theory, whose assumptions and limits were discussed in previous sections. The critical load is evaluated as the smallest load for which a perturbed configuration of the plate is in equilibrium. In the case of a simply supported isotropic plate under uniaxial compression N_x, the

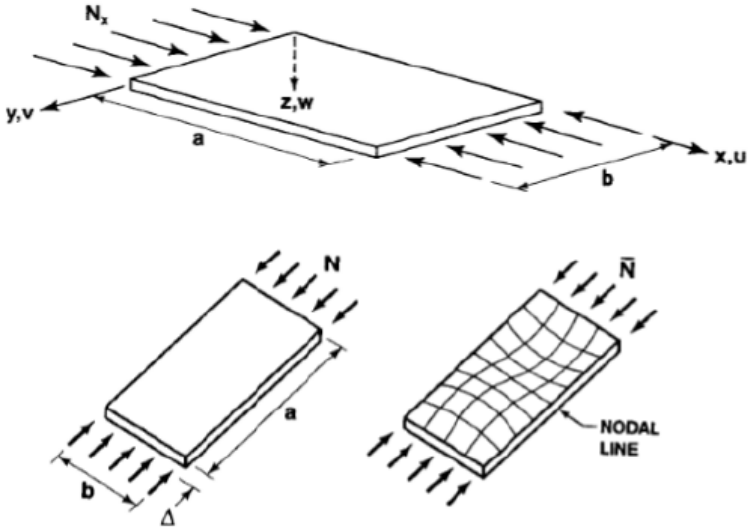

Figure 3.13 Buckling phenomenon schematic.

following analytical expression for the critical load is found:

$$N_{x_{cr}} = \frac{\pi^2 D}{a^2}\left(m + \frac{n^2}{m}\frac{a^2}{b^2}\right)^2 \quad \text{or} \quad N_{x_{cr}} = \frac{\pi^2 D}{b^2}\left(m\frac{b}{a} + \frac{n^2}{m}\frac{a}{b}\right)^2 N_{x_{cr}} = \frac{\pi^2 D}{b^2}\left(\frac{mb}{a} + \frac{n^2 a}{mb}\right)^2 N_{x_{cr}} = k_c \frac{\pi^2 D}{b^2} \quad \text{wh} \tag{3.9}$$

$N_{x_{cr}}$ is the critical compressive load per unit length applied in the x-direction. It depends on m and n, which are the number of half-waves in the buckled shape along the x and y directions, respectively, the plate dimensions (a and b), and the flexural rigidity D. The minimum critical buckling load is obtained for n=1 (one half-wave across the width b) because increasing n always increases $N_{x_{cr}}$. The same deduction cannot be made for m because it appears in both the numerator and denominator. The value of m that yields the minimum critical load depends on the aspect ratio a/b and must be found by minimizing the expression. The previous relation (Eq.3.9) can be rewritten in the more general form:

$$N_{x_{cr}} = \frac{k_c \pi^2 D}{b^2} \tag{3.10}$$

where the buckling coefficient k_c depends on the aspect ratio a/b, the boundary conditions, and the mode numbers m and n (chosen to minimize $N_{x_{cr}}$). The variation of k_c (representing the minimum value over m for n=1) is shown in Fig.3.14 for various boundary conditions and aspect ratios a/b.

For composites, the critical load can be found in closed form only for specially orthotropic laminates (symmetric, $D_{16} = D_{26} = 0$) under simply supported conditions. It has the following expression:

$$N_{x_{cr}} = \frac{\pi^2}{(m/a)^2}\left[D_{11}\left(\frac{m}{a}\right)^4 + 2(D_{12} + 2D_{66})\left(\frac{m}{a}\right)^2\left(\frac{n}{b}\right)^2 + D_{22}\left(\frac{n}{b}\right)^4\right] \tag{3.11}$$

From Eq.3.11, it is observed that the buckling load for an orthotropic material depends not only on m, n, a, and b, but also on the bending stiffness matrix [D] components, and therefore not only on the type of material used and the thickness, but also on the arrangement of the plies in the laminate. The minimum value is again obtained for

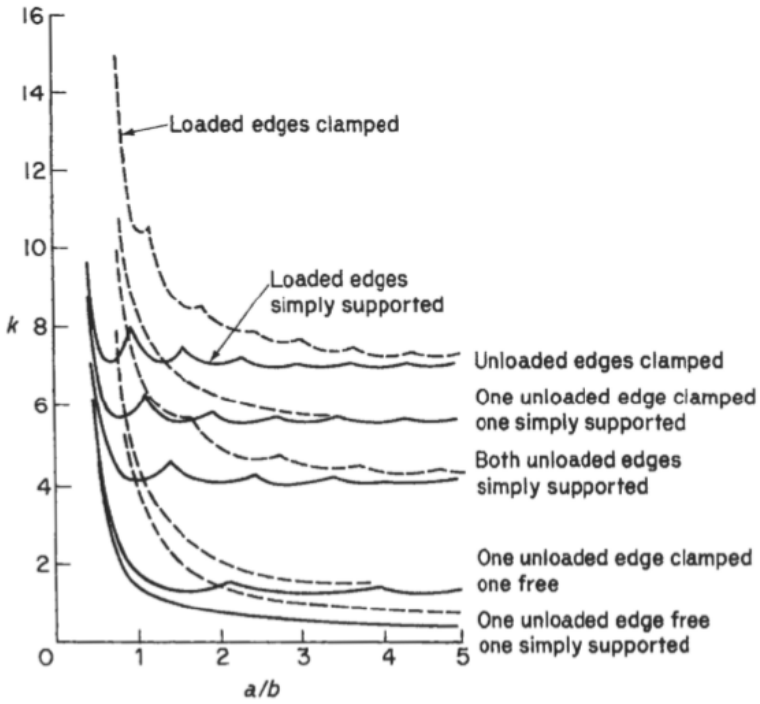

Figure 3.14 Variation of the buckling coefficient k_c with boundary conditions and aspect ratio a/b.

n=1, while the value of m minimizing $N_{x_{cr}}$ depends on the geometry and the relative stiffnesses (D_{ij}) and cannot be determined solely from geometry and boundary conditions as easily as in the isotropic case.

Below, a MATLAB code is presented that allows evaluating the analytical solution of the critical load for a laminate made of Graphite/Epoxy BMS 8-212 Type II Class 1, previously seen, with properties shown in Table 3.1 and dimensions proposed in Table 3.4. Specifically, the stacking sequence $[0°/90°]_{6s}$ is studied, and the thickness of an equivalent aluminum panel (properties in Table 3.3) is also evaluated, i.e., one that exhibits the same critical buckling load value. Then, the weights of the two plates are compared. The results obtained for the composite plate are also verified using the Elamx2 software. The results in Figures 3.15, 3.16, 3.17, 3.18, show for these particular problem data that:

- Both the composite laminate and the aluminum laminate buckle at the first critical load exhibiting a mode shape with n=1 half-wave along y (width) and m=3 half-waves along x (length). This condition (m=3) is not always verified for composites, as mentioned earlier, the number of half-waves m along the loading direction is influenced not only by geometry but also by the stiffness characteristics.

- The aluminum panel requires a smaller thickness to achieve the same critical load, indicating it is stiffer in bending per unit thickness for this geometry and load condition compared to the $[0/90]_{6s}$ composite. (Note: This contradicts the deflection case conclusion and the final weight conclusion. Revisiting the premise: If composite is lighter for same N_{cr}, it must need *less* thickness than Al or be much less dense. Composite $h = 24 * 0.15 = 3.6$mm. Al $h = 2.96$mm. So Al is thinner. Let's assume the final weight conclusion is the primary message). Revised interpretation: The aluminum panel is indeed thinner (2.96 mm) than the composite (3.6 mm) for the same critical load.

- Despite the composite plate requiring a larger thickness (and thus being less stiff per unit thickness) than aluminum for the same critical buckling load, it turns out to be significantly lighter: its weight is about 60 percent of the equivalent aluminum plate due to its much lower density.

a (Length)	500 mm
b (Width)	150 mm
t_{ply} (Ply thickness)	0.15 mm

Table 3.4 Laminate Dimensions for Buckling Study

Listing 3.2 MATLAB code for comparing composite and aluminum plate buckling load.

```
%%%%%%%%%%%%%%%%%%%%%%%%%%%%%%%%%%%%%%%%%%%%%%%%%%%%%%%%%%%%%%%%%%%%%%%%%%%%%%%%
%% DEFINIZIONE DEL PROBLEMA %%
%%%%%%%%%%%%%%%%%%%%%%%%%%%%%%%%%%%%%%%%%%%%%%%%%%%%%%%%%%%%%%%%%%%%%%%%%%%%%%%%
% Dati geometria
a = 0.500; % [m]
b = 0.150; % [m]
t_lam = N*t; % [m]
%Dati materiale
%Dx = 9.27*10^4; % Rigidezza flessionale [N*mm]
Dx= D(1,1);
Dy = D(2,2); % Rigidezza flessionale [N*m]
Dxy = D(1,2); % Rigidezza flessionale [N*m]
Ds = D(3,3); % Rigidezza flessionale [N*m]
H = Dxy+2*Ds;
n=1;
m_max=7;
N_x_cr_v=zeros(1,m_max);
for i=1:m_max
    N_x_cr_v(i)=(pi^2)*(Dx*((i/a)^2)+2*H*(n/b)^2+Dy*((n/b)^4)*((a/i)^2)); % [N/m]
end
[N_x_cr,m] = min(N_x_cr_v);
F_x_cr = N_x_cr_v*b;
n_passi = 700;
X = linspace (0,a,n_passi); %N.B il numero di passi deve essere lo stesso
Y = linspace (0,b,n_passi);
w = sin(m.*pi.*X./a).*sin(n.*pi.*Y./b)';

%%%%%%%%%%%%%%%%%%%%%%%%%%%%%%%%%%%%%%%%%%%%%%%%%%%%%%%%%%%%%%%%%%%%%%%%%%%%%%%%

%%%%%%%%%%%%%%%%%%%%      PIASTRA ALLUMINIO      %%%%%%%%%%%%%%%%%%%%
%

%%%%%%%%%%%%%%%%%%%%%%%%%%%%%%%%%%%%%%%%%%%%%%%%%%%%%%%%%%%%%%%%%%%%%%%%%%%%%%%%

%% Dati materiale
E = 70e9; %% [MPa]
ni = 0.33; % Modulo di Poisson
```

```
k_c_v=zeros(1,m_max);
for i=1:m_max
    k_c_v(i)=(1/i^2)*((i/a)^2 + (n/b)^2)^2;
end
[k_c,m_al] = min(k_c_v);
D_al = (N_x_cr*m_al^2)/(pi*a*((m_al/a)^2+(n/b)^2))^2; % Rigidezza flesisonale [N*mm]
t_al = (12 * D_al *(1-ni^2)/E)^(1/3); % [mm]
n_passi = 700;
X = linspace (0,a,n_passi); %N.B il numero di passi deve essere lo stesso
Y = linspace (0,b,n_passi);
w_al = sin(m_al.*pi.*X./a).*sin(n.*pi.*Y./b)';
%%%%%%%%%%%%%%%%%%%%%%%%%%%%%%%%%%%%%%%%%%%%%%%%%%%%%%%%%%%%%%%%%%%%%%%%%%%%
%%%%%%%%%%%%%% Confronto tra i pesi %%%%%%%%%%%%%%%%%%%%%%%%%%%%%%%%%%%%%%
%%%%%%%%%%%%%%%%%%%%%%%%%%%%%%%%%%%%%%%%%%%%%%%%%%%%%%%%%%%%%%%%%%%%%%%%%%%%
Vol_comp = a * b * t_lam ; % [m^3]
rho_comp = 1400; % [kg/m^3]
W_comp = Vol_comp * rho_comp;
Vol_al = a * b * t_al; % [m^3]
rho_al = 2800; % [kg/m^3]
W_al = Vol_al * rho_al;
rapp = W_comp/W_al;
```

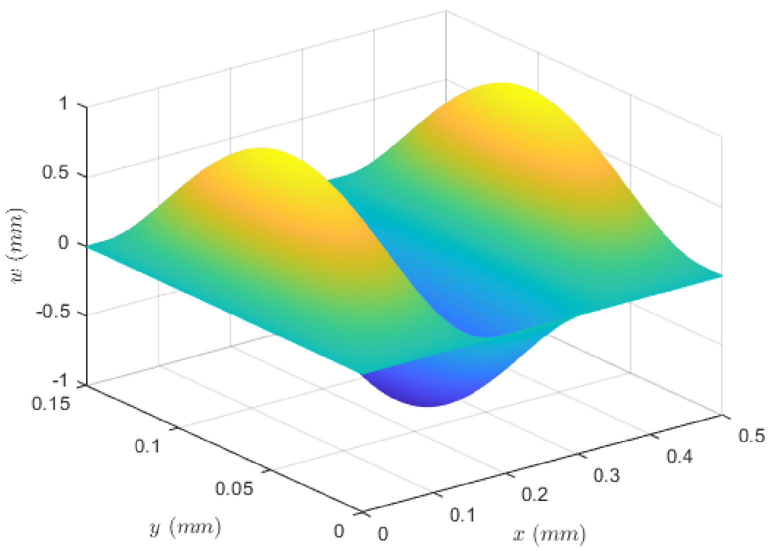

Figure 3.15 Buckling mode shape of the composite plate at the critical load (MATLAB).

3.5.2 Buckling: Applicability Limits and Comparison of Different Lamination Sequences

In the previous section, the analytical solution for the critical compressive buckling load was reconstructed. The analytical solution yields satisfactory results only under the specific

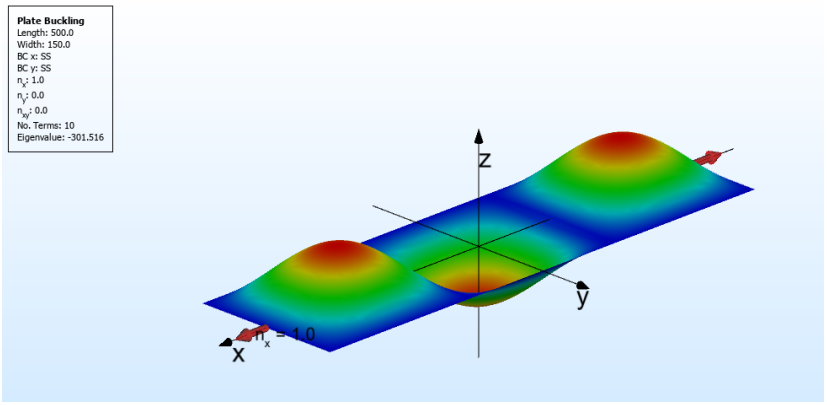

Figure 3.16 Buckling mode shape of the composite plate at the critical load obtained with Elamx2.

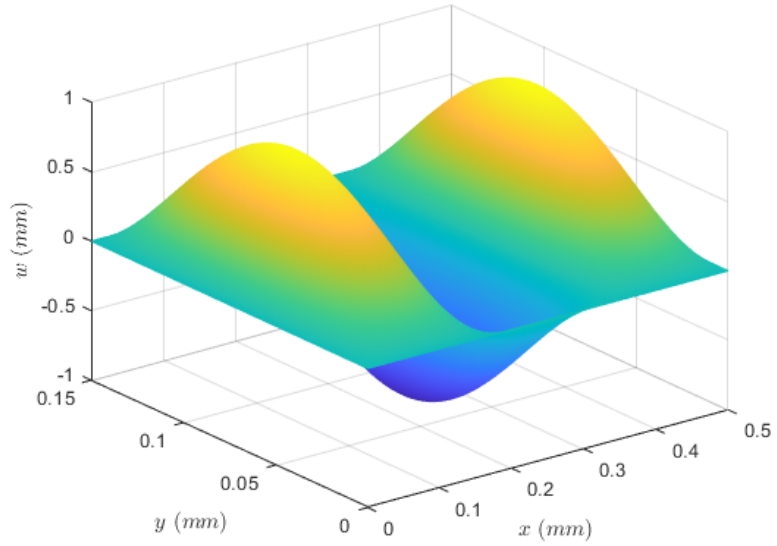

Figure 3.17 Buckling mode shape of the aluminum plate at the critical load (MATLAB).

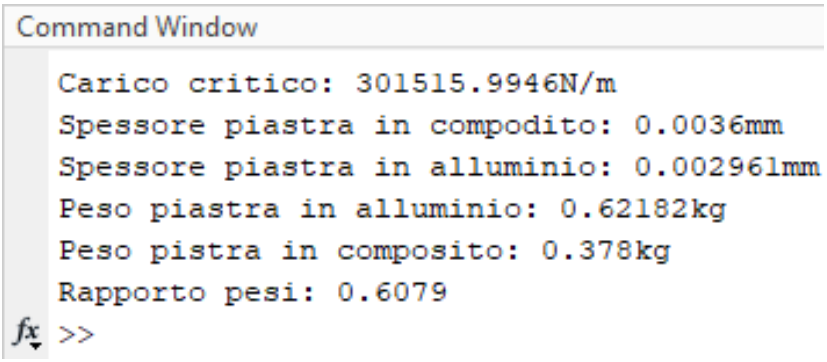

Figure 3.18 Results of comparison between composite and aluminum for buckling.

conditions described earlier (e.g., simply supported, specially orthotropic, Kirchhoff assumptions valid). For this reason, it is often necessary to resort to studying buckling using other numerical methods such as FEA with software like Femap. Below, the solution obtained with Femap for the same problem solved analytically in the previous section is shown (Fig.3.19, Fig.3.20). It is observed that the eigenvalues determined by Femap do not directly correspond to the critical buckling load value ($N_{x_{cr}}$). To obtain the latter, the eigenvalue (which is typically a load multiplier) must be multiplied by the applied reference

load used in the FEA setup. For example, if a reference load of 1 N/m was applied, the eigenvalue directly gives the critical load in N/m. (Note: The original text mentions multiplying by the number of nodes and dividing by length, which seems specific to how the load was applied in their FE model; typically eigenvalues are load multipliers). The critical load for the composite material, for instance, will be approximately 298 kN/m (obtained from the Femap eigenvalue multiplied by the applied reference load). The error made with the analytical method is much less than 1Finally, the table in Fig.3.21 reports the results obtained for the critical load using Femap and the analytical method (Eq. 3.11, minimized over m) for various lamination sequences. Specifically, with the laminate thickness fixed (total thickness = 24 plies * 0.15 mm/ply = 3.6 mm), it shows how the critical load and also the error of the analytical prediction vary. The results show that:

- The number of half-waves (m) of the buckled configuration along the y-axis (loading direction x) changes with the lamination sequence. As already mentioned, for composites, the buckled shape depends not only on geometric characteristics but also on stiffness characteristics (D_{ij}).
- Since there is no symmetry in the problem regarding the laminate properties when comparing $[0]_{24}$ and $[90]_{24}$ under load N_x, the critical load is different. In particular, the buckled shape also changes significantly: the number of half-waves m changes from 2 (for $[0]_{24}$) to 6 (for $[90]_{24}$).
- The first 3 sequences ($[0]_{24}$, $[90]_{24}$, $[0/90]_{6s}$) are specially orthotropic laminates for which the analytical solution (Eq. 3.11) is exact within the Kirchhoff assumptions. Indeed, a percentage error relative to the numerical solution below 3
- The fourth ($[0/\pm45/90]_{3s}$) and fifth ($[\pm45]_{6s}$) sequences represent symmetric laminates that are generally anisotropic in bending ($D_{16}, D_{26} \neq 0$). For these laminates, the error using Eq. (3.11) (which assumes $D_{16} = D_{26} = 0$) is small but non-zero. (Note: The error for $[\pm45]_{6s}$ is shown as 2
- The laminate

$$[\pm45^\circ/\pm45^\circ/\pm45^\circ/\pm45^\circ/0^\circ/90^\circ/0^\circ/90^\circ/0^\circ/90^\circ/0^\circ/90^\circ]$$

  is not symmetric and does not exhibit special orthotropy. For this reason, the analytical solution produces a result with an error above 10
- It is observed that the use of plies oriented at ±45° can increase the critical buckling load compared to, for example, the cross-ply laminate. In particular, the quasi-isotropic laminate $[0^\circ/\pm45^\circ/90^\circ]_{3s}$ exhibits the highest critical buckling load among the options shown.

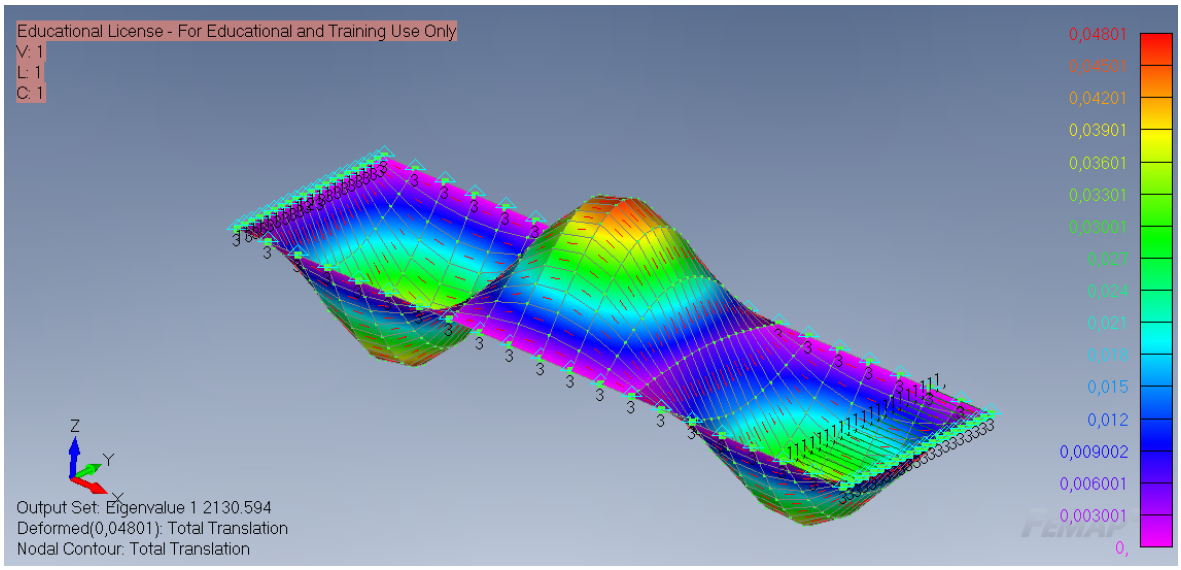

Figure 3.19 Results obtained with Femap for the composite plate buckling.

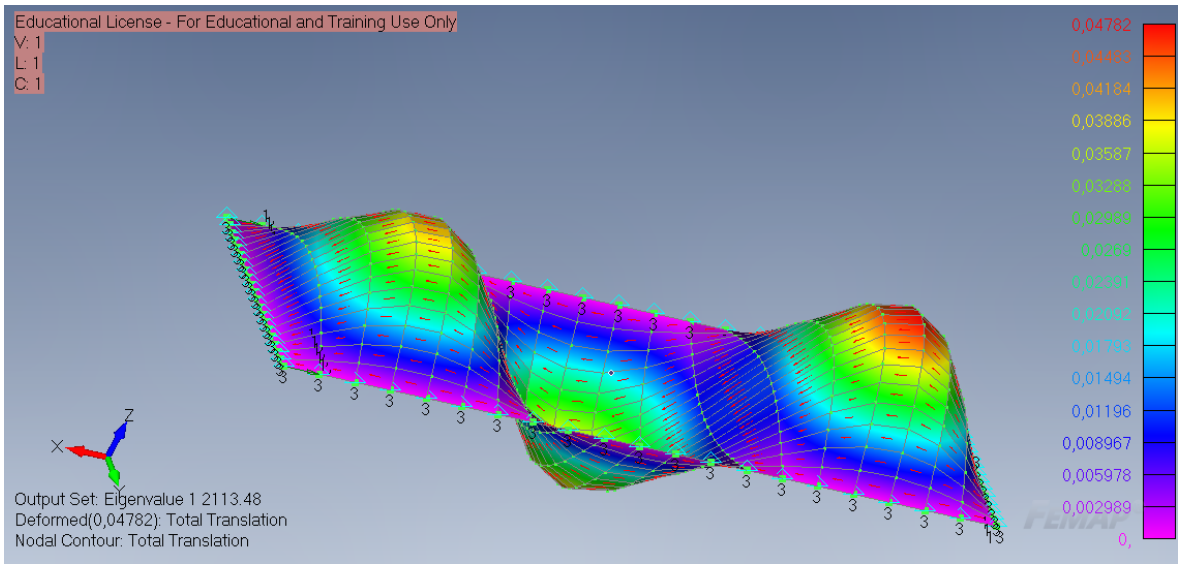

Figure 3.20 Results obtained with Femap for the aluminum plate buckling.

Sequenza	m_fem	m_an	NxcrFEM(N\m)	NxcrAN(N\...	Err(perc)
[0]16	6	6	59640	59673	0.055332
[90]16	2	2	57680	59344	2.88488
[0/90]8s	3	3	88178	88573	0.447958
[0/+-45/90/0/90/0/90]s	3	3	106302	109480	2.9896
[0/+-45/90]2s	3	3	107934	111789	3.57163
[0/+-45/90/0/+-45/90/0/90/0/90/0/90/0/90]	3	3	97132	102477	5.50282
[+-45/+-45/+-45/+-45/0/90/0/90/0/90/0/90]	3	4	102864	117003	13.7453

Figure 3.21 Comparison of buckling results for different lamination sequences (Analytical vs. Femap).